(12) INTERNATIONAL APPLICATION PUBLISHED UNDER THE PATENT COOPERATION TREATY (PCT)

(19) World Intellectual Property Organization
International Bureau

(43) International Publication Date
03 June 2021 (03.06.2021)

WIPO | PCT

(10) International Publication Number
WO 2021/102565 A1

(51) International Patent Classification:
C01G 51/00 (2006.01) *C01G 37/14* (2006.01)
B01J 37/02 (2006.01) *F01N 3/28* (2006.01)
B01J 37/08 (2006.01) *F23C 13/08* (2006.01)

(21) International Application Number:
PCT/CA2020/051603

(22) International Filing Date:
25 November 2020 (25.11.2020)

(25) Filing Language: English

(26) Publication Language: English

(30) Priority Data:
62/940,773 26 November 2019 (26.11.2019) US

(71) Applicant: **THE UNIVERSITY OF BRITISH COLUMBIA** [CA/CA]; #103 - 6190 Agronomy Road, Vancouver, British Columbia V6T 1Z3 (CA).

(72) Inventors: **MACLACHLAN, Mark**; c/o #103 - 6190 Agronomy Road, Vancouver, British Columbia V6T 1Z3 (CA). **WOLF, Michael**; c/o #103 - 6190 Agronomy Road, Vancouver, British Columbia V6T 1Z3 (CA). **SMITH, Kevin**; c/o #103 - 6190 Agronomy Road, Vancouver, British Columbia V6T 1Z3 (CA). **DAI, Yiling**; c/o #103 - 6190 Agronomy Road, Vancouver, British Columbia V6T 1Z3 (CA).

(74) Agent: **SMART & BIGGAR LLP**; 2300-1055 West Georgia Street, PO Box 11115, Vancouver, V6E 3P3 (CA).

(81) Designated States *(unless otherwise indicated, for every kind of national protection available)*: AE, AG, AL, AM, AO, AT, AU, AZ, BA, BB, BG, BH, BN, BR, BW, BY, BZ, CA, CH, CL, CN, CO, CR, CU, CZ, DE, DJ, DK, DM, DO, DZ, EC, EE, EG, ES, FI, GB, GD, GE, GH, GM, GT, HN, HR, HU, ID, IL, IN, IR, IS, IT, JO, JP, KE, KG, KH, KN, KP, KR, KW, KZ, LA, LC, LK, LR, LS, LU, LY, MA, MD, ME, MG, MK, MN, MW, MX, MY, MZ, NA, NG, NI, NO, NZ, OM, PA, PE, PG, PH, PL, PT, QA, RO, RS, RU, RW, SA, SC, SD, SE, SG, SK, SL, ST, SV, SY, TH, TJ, TM, TN, TR, TT, TZ, UA, UG, US, UZ, VC, VN, WS, ZA, ZM, ZW.

(84) Designated States *(unless otherwise indicated, for every kind of regional protection available)*: ARIPO (BW, GH, GM, KE, LR, LS, MW, MZ, NA, RW, SD, SL, ST, SZ, TZ, UG, ZM, ZW), Eurasian (AM, AZ, BY, KG, KZ, RU, TJ,

WO 2021/102565 A1

(54) Title: COBALT CHROMITE NANOPARTICLES, METHODS OF THEIR PREPARATION AND USES THEREOF

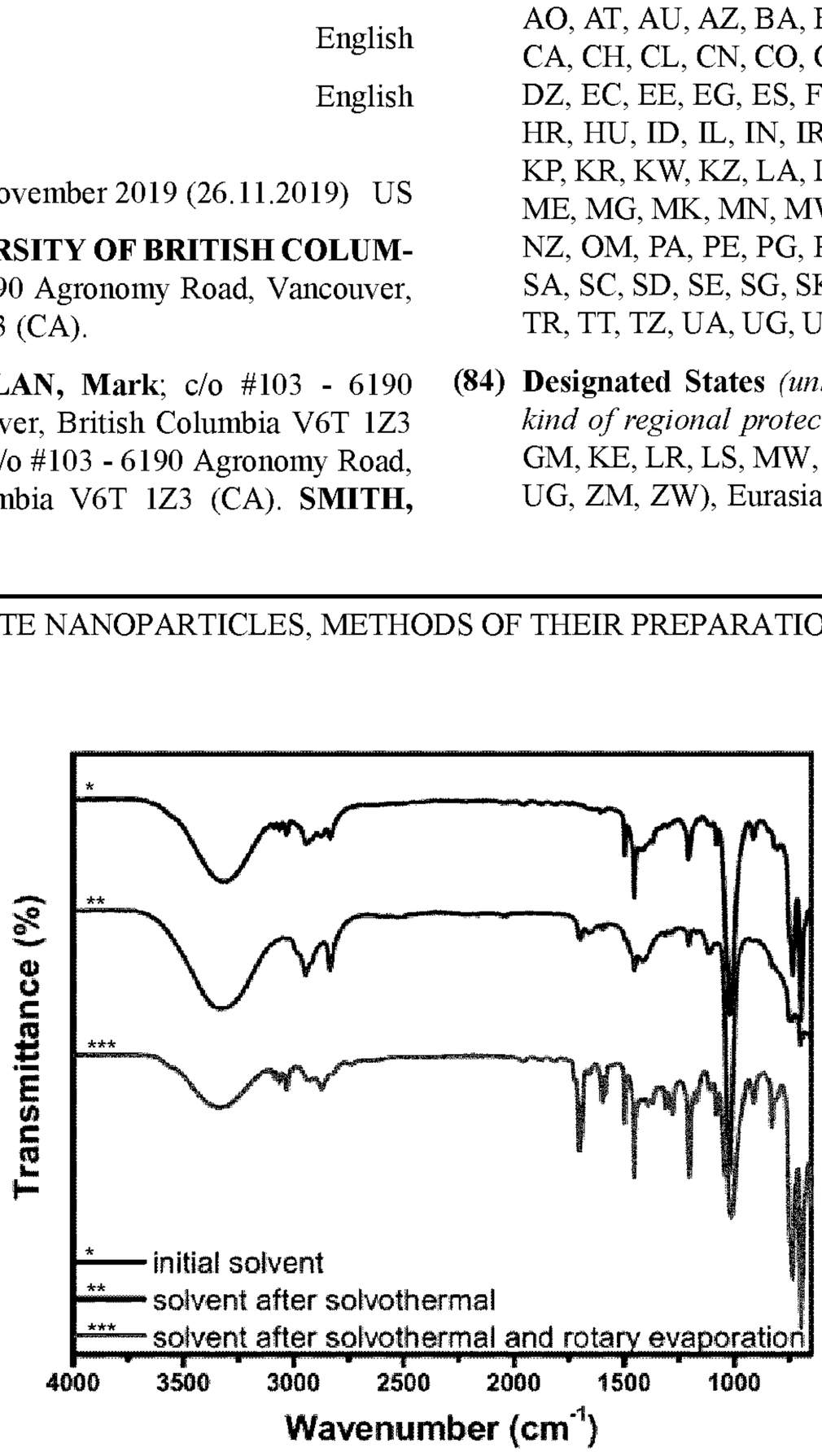


FIG. 1

(57) Abstract: $CoCr_2O_4$ nanoparticles having a Brunauer-Emmett-Teller (BET) specific surface area at 77 K of at least 50 m^2/g are provided which are well suited as catalysts for low temperature methane combustion, even in the presence of water vapor and SO_2. Also provided is a solvothermal method of production of such nanoparticles using an alcohol.

[Continued on next page]

TM), European (AL, AT, BE, BG, CH, CY, CZ, DE, DK, EE, ES, FI, FR, GB, GR, HR, HU, IE, IS, IT, LT, LU, LV, MC, MK, MT, NL, NO, PL, PT, RO, RS, SE, SI, SK, SM, TR), OAPI (BF, BJ, CF, CG, CI, CM, GA, GN, GQ, GW, KM, ML, MR, NE, SN, TD, TG).

Published:

— *with international search report (Art. 21(3))*

— *in black and white; the international application as filed contained color or greyscale and is available for download from PATENTSCOPE*

COBALT CHROMITE NANOPARTICLES, METHODS OF THEIR PREPARATION AND USES THEREOF

CROSS-REFERENCE TO RELATED APPLICATIONS

[001] The present disclosure claims the benefit of priority from co-pending U.S. provisional application no. 62/940,773 filed on November 26, 2019, the contents of which are incorporated herein by reference in their entirety.

FIELD

[002] The present disclosure relates to $CoCr_2O_4$ nanoparticles, methods for the preparation of such nanoparticles and their use, for example, as catalysts for catalytic combustion of methane.

BACKGROUND

[003] Natural gas is an abundant resource with world-wide reserves estimated at 10200 to 15400 trillion cubic feet by the US Geological survey.[1] Importantly, combustion of natural gas produces less pollution (CO_2, NO_x, SO_x) per unit energy delivered than either gasoline or diesel,[2,3] making natural gas vehicles (NGVs) attractive alternatives to help mitigate the effects of climate change by reducing vehicular CO_2 emissions. NGVs, however, have a significant limitation: unburned methane (CH_4) in the exhaust is a greenhouse gas that is about 20 times more potent than CO_2.[4] Without post-engine treatment, a lean-burn natural gas bus may, for example emit a substantially higher amount of CH_4/kWh on the European Stationary Cycle (ESC)[5] than the limit of 0.5 g/kWh mandated by the Euro VI standards for heavy-duty engines.[6] Therefore, to meet current standards, the emission of methane from such engines typically must be significantly reduced.

[004] In gasoline fueled automobiles, 3-way catalytic convertors are used to treat exhaust to remove SO_x, NO_x, and to oxidize CO and hydrocarbons. Unfortunately, methane oxidation in the exhaust of NGVs is a much more challenging prospect owing to the lower temperature of the exhaust stream of NGVs (typically less than 500°C), as well as the low concentration (about 1000 ppm) and high stability of methane.[7] In addition, catalysts desirably remain active in the presence of water vapor, SO_x, and NO_x. For at least these reasons, there is a need for stable catalysts that can oxidize methane at NGV exhaust temperatures.

[005] Supported noble metal catalysts can show outstanding performance for heterogeneous catalytic combustion,[8] and they have been the focus of significant research to develop new low temperature methane-oxidation catalysts. Pd-based catalysts in particular exhibit excellent catalytic activity for this reaction,[9-11] but low hydrothermal stability of these materials has limited their application.[12] In the presence of water vapor, the

adsorption of hydroxyl groups on the support and PdO inhibits the catalytic reaction.[13] Furthermore, Pd is sensitive to the presence of SO_x,[14] leading to irreversible deactivation of the catalyst, and the joint effect of H_2O and SO_2 significantly inhibits the catalytic activity.[15,16] However, incorporation of Au[17,18] or Pt[19,20], or modification of the oxide support[9,21,22,36] in Pd-based catalysts has been shown to enhance stability. Nevertheless, cost and scarcity remain significant factors against the use of precious metals in such catalysts.

[006] Over the past decade, there has been significant interest in the development of nanostructured catalysts based on non-noble metals.[23,24] Transition metal oxides such as Co_3O_4 nanocatalysts have shown catalytic activities comparable to Pd-based catalysts.[25,26] For example, Hu, L. *et al.*[27] studied the effects of crystallite and crystal planes of Co_3O_4 on methane combustion and found that the predominantly exposed {112} planes in Co_3O_4 nanosheets (as compared to nanocubes and nanowires) exhibited the best catalytic activity, achieving 50% conversion ($T_{50\%}$) at 313 °C [gas hourly space velocity (GHSV) = 40000 mL g^{-1} h^{-1}]. Sun, Y. *et al.*[28] explored the effect of different architectures of Co_3O_4 on methane combustion and found that nanoplates resulted in the highest activity with $T_{50\%}$ at 263 °C (GHSV = 10000 mL g^{-1} h^{-1}) as compared to nanoparticles, nanorods and 3-dimensional micro/meso porous structures. Unfortunately, at higher temperatures or in the presence of water, the catalytic activity for Co_3O_4 decreases substantially.

[007] Ordonez, S. *et al.*[29] explored the use of numerous metal oxides for methane oxidation and reported that Cr_2O_3 shows the best stability for methane combustion in real emission conditions containing water and other gases that typically deactivate catalysts. However, the catalytic activity of Cr_2O_3 is not competitive with noble metal catalysts.

[008] Conoco, Inc.[37] disclosed $CoCr_2O_4$ dispersed in a Cr_2O_3 matrix as a catalyst for partial oxidation of methane to produce CO and H_2 for use in hydrocarbon synthesis. Good activity at 630 °C or more was reported but only for catalysts prepared by a sol-gel method with freeze-drying, followed by calcination.

[009] $CoCr_2O_4$ spinel-type oxide catalysts, synthesized by sol-gel or co-precipitation methods have also been applied to methane combustion. For example, Hu, J. *et al.*[30] prepared 2-4.5 μm sized $CoCr_2O_4$ polyhedrons (BET specific surface area of 0.4 m^2/g) by an aqueous glucose sol-gel method followed by calcination and which showed 90% conversion of methane to CO_2 at 750 °C (GHSV = 48,000 h^{-1}). Chen, J. *et al.*[31] prepared a series of single and mixed metal oxides with different Co/Cr ratios by co-precipitation from aqueous ammonia and evaluated them for methane combustion. $CoCr_2O_4$ (BET specific surface area = 38.6 m^2/g) showed the

best catalytic activity with 90% conversion at 464 °C (GHSV = 36,000 h^{-1}). However, the presence of water vapor and SO_2 significantly reduced its catalytic activity.

[010] A wide variety of methods and reagents are known for production of structured metal containing catalysts. The literature shows that the results using the same or different chemical compositions is unpredictable in terms of catalyst structure at the nano-level and surface area, which are factors that can greatly affect catalytic performance. By way of example, Niederberger, M. *et al.*[32] employed a solvothermal approach with various transition metal oxides precipitated from a benzyl alcohol medium and obtained different nanostructures (particles, rods and plates) depending on the metal. Hu, J. *et al.*[33] used a solvothermal approach for nickel oxide using a medium containing methanol and obtained holey nanosheets only when benzyl alcohol was also present. Dai, Y. *et al.*[38] obtained different shaped structures of $NiCo_2O_4$ with a hydrothermal approach using different amines to cause precipitation. Bow-tie shaped crystals made up of $NiCo_2O_4$ nanoplates that were precipitated using oleylamine had a surface area of as much as 65 m^2/g. and demonstrated 100% methane combustion at as low as 410 °C.

[011] Regarding Co_3O_4, the different processes employed by Hu, L. *et al.*[27] and Sun, Y. *et al.*[28] resulted in a range of 0-3 dimensional nanostructures with 2-dimensional (2-D) nanoplates or nanosheets being the best for methane combustion. Using a solvothermal approach with methanol alone or methanol plus benzyl alcohol, Chen, L. *et al.* and Wei, R. *et al.* obtained holey Co_3O_4 nanosheets catalytically active for methanol decomposition[34] or suitable for use as an anode[35].

[012] The literature discussed above suggests that for low-temperature methane combustion, nanostructures comprising 2-D sheets or plates would work best, possibly because of their exposure of high-index {112} planes.

SUMMARY

[013] The present disclosure provides novel $CoCr_2O_4$ nanoparticles as well as methods for preparing such $CoCr_2O_4$ nanoparticles. The nanoparticles can be polycrystals with an extremely large surface area and are surprisingly suited for low temperature methane combustion even in the presence of water vapor and/or SO_2. Improvements in activity for methane combustion over previous $CoCr_2O_4$ catalysts may be as much as a 100 °C decrease for 50% conversion ($T_{50\%}$). The nanoparticles can be generally spherical (zero dimensional) polycrystals and composed of relatively small crystallites. The nanoparticles can be generally smooth and substantially free of any adherent Co_3O_4 nanostructures.

[014] Accordingly, the present disclosure includes a method of preparing $CoCr_2O_4$ nanoparticles, the method comprising: heating a solution of a cobalt (II) compound and a chromium (III) compound in an alcohol to form a precipitate; separating the precipitate from the solution; and calcining the precipitate to form the $CoCr_2O_4$ nanoparticles.

[015] In an embodiment, the alcohol comprises a C_{1-7}alcohol or mixture thereof. In another embodiment, the C_{1-7}alcohol or mixture thereof is methanol. In another embodiment, the alcohol comprises an alcohol that is a reducing agent and a structure-directing agent. In another embodiment, the alcohol that is a reducing agent and a structure-directing agent is an aromatic alcohol. In a further embodiment, the alcohol that is a reducing agent and a structure-directing agent is benzyl alcohol. In another embodiment of the present disclosure, the alcohol is a mixture of methanol and benzyl alcohol.

[016] In an embodiment, the heating of the solution is carried out at a pressure greater than ambient pressure. In another embodiment, the greater than ambient pressure is provided by heating the solution in a sealed environment.

[017] In an embodiment, the heating is at a temperature of about 140 °C to about 200 °C. In another embodiment, the heating is at a temperature of about 180 °C.

[018] In an embodiment, the heating is for a time of about 1 hour to about 24 hours. In another embodiment, the heating is for a time of about 8 hours.

[019] In an embodiment, the cobalt (II) compound and the chromium (III) compound are salts soluble in the alcohol. In another embodiment, the cobalt (II) compound and the chromium (III) compound are nitrate salts. In a further embodiment, the cobalt (II) compound is cobalt (II) nitrate hexahydrate and the chromium (III) compound is chromium (III) nitrate nonahydrate.

[020] In an embodiment, the method further comprises washing the separated precipitate prior to the calcining. In another embodiment, the method further comprises drying the separated and optionally washed precipitate prior to the calcining.

[021] In an embodiment, the calcining is at a temperature of about 400 °C to about 600 °C. In another embodiment, the calcining is at a temperature of about 500 °C.

[022] In an embodiment, the calcining is for a time of about 1 hour to about 15 hours. In another embodiment, the calcining is for a time of about 3 hours.

[023] Also provided are $CoCr_2O_4$ nanoparticles prepared by such a method. In an embodiment, the nanoparticles have a BET specific surface area of at least 90, 95 or 100 m^2/g. In another embodiment, the nanoparticles are generally spherical. In a further

embodiment, the nanoparticles have a diameter of about 300 nm to about 900 nm. In another embodiment, the nanoparticles are polycrystals having a crystallite size of about 6 nm to about 12 nm. In another embodiment, the nanoparticles are polycrystals having a crystallite size of about 10 nm. In a further embodiment, the nanoparticles are generally smooth and substantially free of adhered Co_3O_4 nanostructures. In another embodiment, the nanoparticles are generally smooth and substantially free of Co_3O_4 and Cr_2O_3. Also provided is the use of such nanoparticles as a catalyst for combustion of methane.

[024] The present disclosure also includes a method for catalytic combustion of methane comprising contacting a gaseous stream containing methane and oxygen with a catalyst comprising the nanoparticles of the present disclosure. In an embodiment, the temperature during the contacting is in a range of from about 20 °C to about 600 °C. In another embodiment, the temperature is less than about 500 °C. In another embodiment, the gaseous stream further comprises one or more of water vapor and SO_x. In another embodiment, the catalyst is present in a catalytic converter. In an embodiment, the catalytic converter is in a vehicle and the gaseous stream is the exhaust of the vehicle. In another embodiment, the vehicle is fueled by natural gas. In an alternative embodiment, the catalytic converter is in a stationary power generator and the gaseous stream is the exhaust of the stationary power generator. In another embodiment, the stationary power generator is fueled by natural gas.

[025] The present disclosure also includes a supported catalyst comprising a solid catalyst support; and a coating comprising the nanoparticles of the present disclosure. In an embodiment, the support comprises a bed of alumina, silica, silicon carbide, metal oxide, ceramic, or steatite particles or pellets. In another embodiment, the support is a monolithic ceramic support. In a further embodiment, the monolithic ceramic support comprises cordierite. In an alternative embodiment, the support is a corrugated metal foil. In some embodiments, the support forms a honeycomb structure. In another embodiment, the coating further comprises a secondary support. In an embodiment, the secondary support comprises alumina. Also provided is a catalytic converter comprising such a supported catalyst.

[026] In another aspect, the present disclosure provides a method of preparing $CoCr_2O_4$ nanoparticles, the method comprising: heating a solution of a cobalt (II) compound and a chromium (III) compound in at least one alcohol to form a precipitate comprising cobalt and chromium alkoxides, carboxylates, or both alkoxides and carboxylates; separating the precipitate from the solution; and calcining the precipitate to form the $CoCr_2O_4$ nanoparticles. The heating step is a solvothermal process and the duration of heating represents the solvothermal reaction time. The $CoCr_2O_4$ nanoparticles can be generally spherical (0-D) polycrystals with a Brunauer-Emmett-Teller (BET) specific surface area at 77 K of at least 50

m^2/g. The $CoCr_2O_4$ nanoparticles can have diameters from about 300 nm to about 900 nm. In some embodiments, the specific surface area is at least about 90, 95 or 100 m^2/g. The $CoCr_2O_4$ nanoparticles can be generally smooth and substantially free of adhered Co_3O_4 nanostructures. The solution may be under pressure during the heating. Such pressure may be provided by maintaining the solution in a sealed environment during the heating. The heating may be at about 140 °C to about 200 °C and in particular embodiments, the heating is at about 180 °C. The heating may be for a time sufficient for the precipitate to become substantially free of Co_3O_4 and Cr_2O_3 and/or for the $CoCr_2O_4$ nanoparticles to be substantially free of adhered Co_3O_4 nanostructures. The heating may be for about 8 hours to about 24 hours or more. The at least one alcohol may comprise a C_1-C_7 alcohol. The at least one alcohol may comprise an aromatic alcohol. At least one alcohol may comprise methanol, ethanol or butanol. The least one alcohol may comprise benzyl alcohol. The at least one alcohol may be a mixture of methanol and benzyl alcohol. The compounds may be cobalt (II) and chromium (III) salts that are soluble in the at least one alcohol and in some embodiments are other than chloride salts, such as cobalt (II) acetate tetrahydrate, and chromium (III) acetate hydroxide, cobalt (II) sulfate heptahydrate, chromium (III) sulfate hydrate, cobalt (II) acetylacetonate, and chromium(III) acetylacetonate. The compounds may be nitrate salts such as cobalt (II) nitrate hexahydrate and chromium (III) nitrate nonahydrate. The separated precipitate may be washed prior to the calcining. The calcining may be at a temperature of about 400 °C to about 600 °C, and in particular embodiments, the calcining is at about 500 °C. The calcining may be for about 3 hours to about 15 hours and in particular embodiments, the calcining is for about 3 hours. Also provided are $CoCr_2O_4$ nanoparticles prepared by such a method.

[027] In another aspect, the present disclosure provides $CoCr_2O_4$ nanoparticles having a Brunauer-Emmett-Teller (BET) specific surface area at 77 K of at least 50 m^2/g. In particular embodiments, the surface area is at least about 90, 95 or 100 m^2/g. The nanoparticles can be generally spherical (zero-dimensional) polycrystals. The nanoparticles can have diameters from about 300 nm to about 900 nm. The nanoparticles can have a crystallite size of about 10 nm (6 - 12 nm). The nanoparticles can be generally smooth and can be substantially free of adhered Co_3O_4 structures. The nanoparticles can be substantially free of any Co_3O_4 or Cr_2O_3. Also provided is the use of such nanoparticles as a catalyst for combustion of methane.

[028] In another aspect, the present disclosure provides a method for catalytic combustion of methane comprising passing a gaseous stream containing the methane and oxygen over a catalyst comprising the aforementioned $CoCr_2O_4$ nanoparticles at an elevated temperature. The temperature may be from about 20 °C to about 600 °C. The catalyst may be present in a catalytic converter. The catalytic converter may be for use with an internal combustion engine.

The internal combustion engine may be fueled at least in part by methane. The catalytic converter may be for a vehicle. The gaseous stream may be the exhaust of a natural gas fueled engine. The exhaust may comprise water vapor. The exhaust may comprise at least 10 vol % water vapor. The exhaust may comprise SO_2. The exhaust may comprise at least 5 ppm SO_2. The catalytic converter may be for a stationary power generator.

[029] In another aspect, the present disclosure provides a solid catalyst support coated with the aforementioned $CoCr_2O_4$ nanoparticles. The support may comprise a bed of alumina, silica, silicon carbide, metal oxide, ceramic, or steatite particles or pellets that are coated with said nanoparticles. The support may be a monolithic ceramic support which may comprise cordierite. The support may be a corrugated metal foil. The support may form a honeycomb structure. The coating may be of the nanoparticles in a carrier which is adhered to the support. Such a carrier may be colloidal alumina adhered to the support by calcining.

[030] In another aspect, the present disclosure provides a catalytic converter comprising a catalyst support and a catalyst comprising the aforementioned $CoCr_2O_4$ nanoparticles. The catalytic converter may be for use with an internal combustion engine. The internal combustion engine may be fueled at least in part by methane. The catalytic converter may be for a stationary power generator. The catalytic converter may be for use in a vehicle. The gaseous stream may be the exhaust of a natural gas fueled vehicle.

[031] In another aspect, the present disclosure provides an exhaust system comprising one or more exhaust conduits and the aforementioned catalytic converter.

[032] In another aspect, the present disclosure provides a stationary power generator comprising the aforementioned catalytic converter.

[033] In another aspect, the present disclosure provides a vehicle comprising the aforementioned catalytic converter.

[034] Other features and advantages of the present disclosure will become apparent from the following detailed description. It should be understood, however, that the detailed description and the specific examples, while indicating embodiments of the disclosure, are given by way of illustration only and the scope of the claims should not be limited by these embodiments, but should rather be given the broadest interpretation consistent with the description as a whole.

BRIEF DESCRIPTION OF THE DRAWINGS

[035] **FIG. 1** shows Fourier-transform infrared (FTIR) spectra for initial solvent (*), solvent after solvothermal process (**) and solvent after solvothermal process and rotary evaporation (***).

[036] **FIG. 2** shows powder X-ray diffraction (PXRD) patterns for $CoCr_2O_4$ precursors prepared with different solvothermal reaction times: 24 h (*), 8 h (**) and 1 h (***) before calcination. (▼) Spinel, *syn*–$Co_{2.74}O_4$ (JCPDS 78-5614).

[037] **FIG. 3** shows FTIR spectra for $CoCr_2O_4$ precursors prepared with different solvothermal reaction times: 24 h (*), 8 h (**) and 1 h (***) before calcination.

[038] **FIG. 4** shows FTIR spectra for $CoCr_2O_4$ precursors prepared without adding benzyl alcohol with different solvothermal reaction times: 24 h (*), 8 h (**) and 1 h (***) before calcination.

[039] **FIG. 5** shows thermogravimetric analysis (TGA) traces for a $CoCr_2O_4$ precursor (**) and a $CoCr_2O_4$ precursor prepared without adding benzyl alcohol (*), each having solvothermal reaction times of 24 h.

[040] **FIG. 6** shows PXRD patterns for $CoCr_2O_4$ nanoparticles prepared with different solvothermal reaction times: from top to bottom, 24 h, 12 h, 8 h, 6 h, 3 h and 1 h. (■) Cobalt chromite, *syn*–$Co_2Cr_2O_4$ (JCPDS 22-1084). (▼) Spinel, *syn*–$Co_{2.74}O_4$ (JCPDS 78-5614). (●) Eskolaite, *syn*–Co_2O_3 (JCPDS 38-1479). The plots are stacked with an offset to make viewing easier.

[041] **FIG. 7** shows enlarged PXRD patterns of those shown in FIG. 6 for $CoCr_2O_4$ nanoparticles prepared with different solvothermal reaction times: from top to bottom, 24 h, 12 h, 8 h, 6 h, 3 h and 1 h. (▼) Spinel, *syn*–$Co_{2.74}O_4$ (JCPDS 78-5614).

[042] **FIG. 8** shows scanning electron microscope (SEM) images of $CoCr_2O_4$ particles prepared with different solvothermal reaction times in methanol plus benzyl alcohol: 1 h (upper left image), 3 h (upper center image), 6 h (upper right image), 8 h (lower left image), 12 h (lower center image), and 24 h (lower right image). Scale bar in all images shows 1 μm.

[043] **FIG. 9** shows high-angle annular dark field (HAADF) images (upper row of images) and energy-dispersive X-ray spectroscopy (EDX) mapping images (lower row of images) for $CoCr_2O_4$ nanoparticles prepared with different solvothermal reaction times: 1 h (images in far left column), 3 h (images in second column from left), 8 h (images in second column from right), and 24 h (images in far right column). Scale bar in all images shows 500 nm.

[044] **FIG. 10** is a SEM image showing $CoCr_2O_4$ prepared with an 8 h solvothermal process. The white arrows point to hollow structures or breakage of Co_3O_4.

[045] **FIG. 11** shows HAADF images (left column) and EDX mapping images (right column) for $CoCr_2O_4$ catalysts prepared without benzoic acid for different solvothermal reaction times: 1 h (images in upper row; scale bars show 100 nm), 8 h (images in center row; scale bars show 500 nm), and 24 h (images in lower row; scale bars show 1 μm).

[046] **FIG. 12** shows high-resolution transmission electron microscopy (HRTEM) images of $CoCr_2O_4$ prepared with different solvothermal reaction times: 1 h (images in upper row), 8 h (images in centre row), and 24 h (images in lower row). The center column shows enlargements of the region designated "1" in the left column. The right column shows enlargements of the region designated "2" in the left column. Scale bars in left column show 300 nm (upper two images) and 500 nm (lower image). Other scale bars in main images show 10 nm.

[047] **FIG. 13** shows X-ray photoelectron spectroscopy (XPS) spectra of Cr 2p (left) and O 1s (right) regions for with $CoCr_2O_4$ prepared with different solvothermal reaction times: 24 h (upper spectra), 8 h (second spectra from top) and 1 h (second spectra from bottom) in comparison to $CoCr_2O_4$ prepared without adding benzyl alcohol with a solvothermal reaction time of 24 h (bottom spectra). The plots are stacked with an offset to make viewing easier.

[048] **FIG. 14** is a graph showing catalytic methane combustion data (methane conversion as a function of temperature, °C) for $CoCr_2O_4$ prepared with different solvothermal reaction times: 1 h, 3 h, 6 h, 8 h, 12 h and 24 h, calcined at 500 °C for 3 h.

[049] **FIG. 15** is a graph showing catalytic methane combustion data (methane conversion as a function of temperature, °C) for the listed nanostructured catalysts.

[050] **FIG. 16** shows Arrhenius plots for the listed nanostructured catalysts.

[051] **FIG.17** is a graph showing catalytic methane combustion data (methane conversion as a function of time, h) for $CoCr_2O_4$ prepared with different solvothermal reaction times: 24 h, 8 h and 1 h, with injection of 10% water and 5 ppm SO_2 at 500 °C.

[052] **FIG. 18** is a graph showing catalytic methane combustion data (methane conversion as a function of temperature, °C) for the listed $CoCr_2O_4$ samples prepared without benzyl alcohol under dry conditions.

[053] **FIG. 19** is a graph showing catalytic methane combustion data (methane conversion as a function of time, h) for the listed $CoCr_2O_4$ samples prepared without benzyl alcohol under wet conditions.

[054] **FIG. 20** shows H_2-temperature programmed reduction (TPR) profiles for the listed catalysts. The plots are stacked with an offset to make viewing easier.

[055] **FIG. 21** shows O_2-temperature programmed desorption (TPD) profiles for the listed catalysts.

[056] **FIG. 22** shows catalytic methane combustion data (methane conversion as a function of time, h) for the $CoCr_2O_4$ catalyst prepared with a solvothermal reaction time of 8 h ($CoCr_2O_{4\ 8h}$) with injection of 10% water and 5 ppm SO_2 at 500 °C over 10 runs.

[057] **FIG. 23** shows an HAADF image (far left) and images showing EDX mapping for Co (second image from left), Cr (second image from right) and Co and Cr (far right image) for $CoCr_2O_{4\ 8h}$ after durability testing. Scale bars in each image show 500 nm.

[058] **FIG. 24** is transmission electron microscopy (TEM) image showing $CoCr_2O_{4\ 8h}$ after durability testing. The arrows point to the sintered Co_3O_4 particles. Scale bar shows 200 nm.

[059] **FIG. 25** shows PXRD patterns for the listed used $CoCr_2O_4$ catalysts. (■) Cobalt chromite, *syn*– $Co_2Cr_2O_4$ (JCPDS 22-1084). (▼) Spinel, *syn*–$Co_{2.74}O_4$ (JCPDS 78-5614). (●) Eskolaite, *syn*–Co_2O_3 (JCPDS 38-1479). (♦) Quartz, syn-SiO_2 (JCPDS 79-1910) (►) Moissanite 4 H-SiC (JCPDS 72-4532). The plots are stacked with an offset to make viewing easier.

[060] **FIG. 26** is a graph showing temperature programmed oxidation (TPO) results (methane conversion as a function of temperature, °C) for a coated monolith catalyst.

DETAILED DESCRIPTION

I. Definitions

[061] Unless otherwise indicated, the definitions and embodiments described in this and other sections are intended to be applicable to all embodiments and aspects of the disclosure herein described for which they would be understood to be suitable by a person skilled in the art.

[062] Terms of degree such as “about” and “approximately” as used herein mean a reasonable amount of deviation of the modified term such that the end result is not significantly changed. These terms of degree should be construed as including a deviation of at least ±5% of the modified term if this deviation would not negate the meaning of the term it modifies.

[063] The term “and/or” as used herein means that the listed items are present, or used, individually or in combination. In effect, this term means that “at least one of” or “one or more” of the listed items is present or used.

[064] When introducing components of the present disclosure or the embodiments thereof, the articles “a”, “an”, “the” and “said” are not intended to exclude there being more than one of the referenced components. In other words, as used in this disclosure, the singular forms “a”, “an”, “the” and “said” include plural references unless the content clearly dictates otherwise.

[065] As used herein, the terms “comprising” (and any form thereof, such as “comprise” and “comprises”), “including” (and any form thereof, such as “include” and “includes”),

"having" (and any form thereof such as "have" and "has") or "containing" (and any form thereof such as "contain" and "contains") are intended to be inclusive or open-ended and mean that there may be additional components other than those listed; i.e. they do not exclude additional, unrecited elements or process/method steps. As used herein, the word "consisting" and its derivatives are intended to be close-ended terms that specify the presence of the stated features, elements, components, groups, integers and/or steps, and also exclude the presence of other unstated features, elements, components, groups, integers and/or steps. The term "consisting essentially of", as used herein, is intended to specify the presence of the stated features, elements, components, groups, integers, and/or steps as well as those that do not materially affect the basic and novel characteristic(s) of these features, elements, components, groups, integers and/or steps.

[066] The terms "generally" and "substantially" as used herein include cases where the referenced characteristic is completely or entirely present.

[067] The term "alkyl" as used herein, whether it is used alone or as part of another group, means straight or branched chain, saturated alkyl groups. The number of carbon atoms that are possible in the referenced alkyl group are indicated by the numerical prefix "C_{n1-n2}". For example, the term C_{1-7}alkyl means an alkyl group having 1, 2, 3, 4, 5, 6 or 7 carbon atoms.

[068] "C_{n1}-C_{n2}alcohol" as used herein refers to an alcohol having from n1 to n2 carbon atoms. For example, a C_1-C_7alcohol is an alcohol having 1, 2, 3, 4, 5, 6 or 7 carbon atoms.

[069] The term "aromatic alcohol" as used herein refers to an alcohol comprising an aryl group. The term "aryl" as used herein, whether it is used alone or as part of another group, refers to cyclic groups that contain at least one aromatic ring. In an embodiment of the application, the aryl group contains from 6, 9, 10 or 14 atoms, such as phenyl.

[070] Nanoparticles of this disclosure may have a diameter greater than 100 nm and thus, the term "nano" in this context is not limited to structures with dimensions of 100 nm or less as may be the case in other fields.

II. Methods of Preparation

[071] Disclosed herein are novel $CoCr_2O_4$ nanoparticles and synthetic methods for the production of such $CoCr_2O_4$ nanoparticles. The nanoparticles are typically zero-dimensional as opposed to 1- or 2-dimensional structures such as rods, plates or sheets.

[072] Accordingly, the present disclosure includes a method of preparing $CoCr_2O_4$ nanoparticles, the method comprising: heating a solution of a cobalt (II) compound and a

chromium (III) compound in an alcohol to form a precipitate; separating the precipitate from the solution; and calcining the precipitate to form the $CoCr_2O_4$ nanoparticles.

[073] The alcohol can be a suitable alcohol or a suitable mixture of alcohols. In an embodiment of the present disclosure, the alcohol comprises a C_1-C_7alcohol or mixture thereof. In another embodiment, the alcohol comprises a C_1-C_7alkyl-OH or mixture thereof. In a further embodiment, the alcohol comprises a C_{1-4}alkyl-OH or mixture thereof. In an embodiment, the C_1-C_4alkyl-OH is methanol, ethanol, butanol or mixtures thereof. In another embodiment, the C_{1-7}alcohol or mixture thereof is methanol. The use of an alcohol that is capable of acting as a reducing agent (such as benzyl alcohol) may facilitate redox reactions of the transition metal ions, enabling the formation of homogeneous mixed oxide structures. Alcohols such as benzyl alcohol may also have a role in controlling the particle size and/or smoothness of the particle surfaces during formation, possibly through surface capping with benzoate groups. Accordingly, in an embodiment of the present disclosure, the alcohol comprises an alcohol that is a reducing agent and a structure-directing agent. the term "reducing agent" as used herein refers to an alcohol capable of losing an electron in a redox reaction during heating with the cobalt (II) compound and the chromium (III) compound in the methods of preparing $CoCr_2O_4$ nanoparticles of the present disclosure. The term "structure-directing agent" as used herein refers to an alcohol capable of guiding and/or influencing aspects of the structure of the $CoCr_2O_4$ nanoparticles in the methods of preparing $CoCr_2O_4$ nanoparticles of the present disclosure. For example, a structure-directing agent may influence aspects such as the nanoparticle size, nanoparticle shape, nanoparticle pore size and/or surface properties of the nanoparticles. In an embodiment, the alcohol that is a reducing agent and a structure-directing agent is an aromatic alcohol. In another embodiment, the aromatic alcohol is benzyl alcohol. In another embodiment, the alcohol is a mixture of a C_{1-7}alcohol or mixture thereof (e.g. a C_1-C_7alkyl-OH or mixture thereof) and an alcohol (e.g. benzyl alcohol) that is a reducing agent and a structure-directing agent. In an embodiment, the alcohol is a mixture of methanol and benzyl alcohol. The molar ratio of methanol to benzyl alcohol can be any suitable ratio. In an embodiment, the molar ratio is from about 5:1 to about 50:1, about 15:1 to about 20:1 or about 17:1. The molar ratio of the alcohol that is a reducing agent and a structure-directing agent (e.g. the benzyl alcohol) to the total amount of the cobalt (II) compound and the chromium (III) compound can be any suitable ratio. In an embodiment, the molar ratio of the alcohol that is a reducing agent and a structure-directing agent (e.g. the benzyl alcohol) to the total amount of the cobalt (II) compound and the chromium (III) compound can be at least about 4.8:1. The molar ratio of the total amount of alcohol to the total amount of the cobalt (II) compound and the chromium (III) compound can be any suitable ratio. In an embodiment, the molar ratio of the total amount of alcohol (e.g. the mixture of

methanol and benzyl alcohol) to the total amount of the cobalt (II) compound and the chromium (III) compound is from about 29:1 to about 245:1, about 70:1 to about 110:1 or about 87:1.

[074] In an embodiment, the solvothermal process is carried out under pressure; i.e. the heating of the solution is carried out at a pressure greater than ambient pressure. A person skilled in the art would readily appreciate that ambient pressure may depend, for example, on the altitude at which the method is being carried out and can readily determine by means in the art what a pressure greater than ambient pressure would be for a particular location (e.g., sea level standard atmospheric pressure is 101325 Pa). The pressure may be created by conducting the solvothermal process in a sealed environment, such as but not limited to an autoclave. Accordingly, in another embodiment, the greater than ambient pressure is provided by heating the solution in a sealed environment.

[075] In an embodiment, the solvothermal process is carried out at a temperature of about 140°C to about 200°C; i.e. the heating is at a temperature of about 140°C to about 200°C. In another embodiment, the heating is at a temperature of about 180°C.

[076] The solvothermal reaction time (i.e. the heating) is for a time suitable to obtain a precipitate that is a $CoCr_2O_4$ precursor. The term "$CoCr_2O_4$ precursor" as used herein refers to the precipitate obtained from the solvothermal reaction between the cobalt (II) compound, chromium (III) compound and the alcohol. A person skilled in the art would readily appreciate that the composition of the $CoCr_2O_4$ precursor will depend, for example, on the identity of the alcohol. For example, when the alcohol comprises a mixture of methanol and benzyl alcohol the $CoCr_2O_4$ precursor may comprise methoxy and/or benzoate groups. Accordingly, the $CoCr_2O_4$ precursor may be a compound or mixture comprising cobalt and chromium alkoxides, carboxylates, or both alkoxides and carboxylates. In an embodiment, the heating is for a time of from about 1 hour to about 24 hours, about 6 hours to about 24 hours or about 8 hours.

[077] The cobalt (II) compound and the chromium (III) compound are any suitable cobalt (II) compound and chromium (III) compound. In an embodiment, the cobalt (II) compound and the chromium (III) compound are salts soluble in the alcohol. In another embodiment, the cobalt (II) compound and chromium (III) compound are other than chloride salts. For example, in some embodiments, the cobalt (II) compound is a cobalt (II) acetate (e.g. cobalt (II) acetate tetrahydrate), a cobalt (II) sulfate (e.g. cobalt (II) sulfate heptahydrate), cobalt (II) acetylacetonate, a cobalt (II) nitrate (e.g. cobalt(II) nitrate hexahydrate) or combinations thereof. In another embodiment, the chromium (III) compound is chromium (III) acetate hydroxide, chromium (III) sulfate hydrate, chromium(III) acetylacetonate, a chromium (III) nitrite (e.g. chromium (III) nitrate nonahydrate) or combinations thereof. In an embodiment, the cobalt

(II) compound and the chromium (III) compound are nitrate salts. In another embodiment, the cobalt (II) compound is cobalt (II) nitrate hexahydrate and the chromium (III) compound is chromium (III) nitrate nonahydrate. The molar ratio of the cobalt (II) compound to the chromium (III) compound can be any suitable ratio. In a embodiment, the molar ratio of the cobalt (II) compound to the chromium (III) compound in the solvothermal process is about 1:2.

[078] The separation of the precipitate from the solution can be carried out using any suitable means, the selection of which can be made by the skilled person. In an embodiment, the separation comprises filtration, optionally with application of suction.

[079] In an embodiment, the method further comprises washing the separated precipitate prior to the calcining. The washing can be carried out using any suitable means, the selection of which can be made by the person skilled in the art. For example, in an embodiment, the washing comprises washing with a suitable solvent (e.g. a low boiling point alcohol such as ethanol), for a suitable number of times (e.g. from 1 to 5, 2 to 4 or 3 times).

[080] In another embodiment, the method further comprises drying the separated and optionally (i.e. where the method comprises washing the separated precipitate) washed precipitate prior to the calcining. The drying can be carried out using any suitable means, the selection of which can be made by the person skilled in the art. For example, in an embodiment, the drying comprises drying at a temperature greater than ambient and lower than the temperature for calcining (e.g. a temperature of from about 160°C to about 200°C or about 180°C) for a suitable time (e.g. about 1 hour to about 4 hours or about 2 hours).

[081] The conditions for calcining are any suitable conditions. For example, a person skilled in the art would readily appreciate that calcination is carried out at high temperatures in the presence of oxygen e.g. from air or another suitable oxygen source. In an embodiment, the precipitate (i.e. the $CoCr_2O_4$ precursor) is calcined at temperature of at least about 400°C, for example, a temperature of about 400°C to about 600°C, about 450°C to about 550°C or about 500°C. The calcining is for any suitable time, for example, a time of about 1 hour to about 15 hours, about 1 hour to about 5 hours or about 3 hours.

[082] The present disclosure also includes a method for preparing $CoCr_2O_4$ nanoparticles comprising heating a solution of a cobalt (II) compound and a chromium (III) compound and at least one alcohol to form a precipitate comprising cobalt and chromium alkoxides, carboxylates, or both alkoxides and carboxylates; separating the precipitate from the solution; and calcining the precipitate to form the $CoCr_2O_4$ nanoparticles.

II. Nanoparticles, Supported Catalysts and Uses

[083] Spinel $CoCr_2O_4$ nanostructured catalysts were prepared by a facile solvothermal method. The growth mechanism of the $CoCr_2O_4$ nanospheres was studied by Fourier-transform infrared (FTIR) spectroscopy and powder X-ray diffraction (PXRD). The influence of solvothermal reaction time on the morphology, structure, and oxidation states of the products was investigated through scanning electron microscopy (SEM), high-resolution transmission electron microscopy (HRTEM), and X-ray photoelectron spectroscopy (XPS). It was found that early in the reaction, the $CoCr_2O_4$ spheres are coated with parasitic Co_3O_4 nanoparticles that disappear after longer reaction times to yield smooth $CoCr_2O_4$ particles.

[084] Accordingly, the present disclosure also includes $CoCr_2O_4$ nanoparticles prepared by a method of preparing $CoCr_2O_4$ nanoparticles of the present disclosure. In an embodiment, the nanoparticles prepared by such a method have a Brunauer-Emmett-Teller (BET) specific surface area at 77 K of at least 50 m^2/g. The present disclosure also includes $CoCr_2O_4$ nanoparticles having a Brunauer-Emmett-Teller (BET) specific surface area at 77 K of at least 50 m^2/g. In an embodiment, the nanoparticles of the present disclosure have a BET specific surface area at 77 K of at least 90, 95 or 100 m^2/g. In an embodiment, the nanoparticles are generally spherical. In another embodiment, the nanoparticles have a diameter of about 300 nm to about 900 nm. In another embodiment, the nanoparticles are polycrystals having a crystallite size of at least 6 nm to about 12 nm. In another embodiment, the polycrystals have a crystallite size of about 10 nm. In an embodiment, the nanoparticles are generally smooth and substantially free of adhered Co_3O_4 nanostructures. In another embodiment, the nanoparticles are generally smooth and substantially free of Co_3O_4 and Cr_2O_3.

[085] The catalytic performance of the noble metal-free nanospheres was optimized for oxidation of methane to CO_2 as evaluated at a high space velocity of 180 000 mL g^{-1} h^{-1}, reaching 100% conversion below 500 °C. Additionally, samples prepared with 8 h solvothermal treatment exhibited excellent stability, maintaining 80% conversion in the presence of 10% H_2O and 5 ppm SO_2 after 10 cycles (about 170 h). The high stability gives these nanomaterials potential for application, for example, in natural gas vehicles.

[086] Accordingly, the present disclosure also includes uses of the nanoparticles of the present disclosure as a catalyst for combustion of methane. The present disclosure also includes a method for catalytic combustion of methane comprising contacting a gaseous stream containing methane and oxygen with a catalyst comprising the nanoparticles of the present disclosure. The contacting can be via any suitable method or means, the selection

of which can be made by a person skilled in the art. In an embodiment, the contacting comprises passing the gaseous stream over the catalyst comprising the nanoparticles.

[087] In an embodiment, the temperature during the contacting is in a range of from about 20°C to about 600°C. In another embodiment, the temperature is at an elevated temperature. In another embodiment, the temperature is less than about 550°C or less than about 500°C.

[088] In an embodiment, the gaseous stream further comprises one or more of water vapor and SO_x. In an embodiment, the gaseous stream further comprises water vapor. In another embodiment, the gaseous stream further comprises at least 1 vol% water vapor. In an embodiment, the gaseous stream further comprises SO_x (e.g. SO_2). In another embodiment, the gaseous stream further comprises at least 1 vol% SO_2 vapor. In some embodiments of the present disclosure, the gaseous stream further comprises NO_x.

[089] A monolith coated with the nanoparticles of the present disclosure was prepared which exhibited very good catalytic activity for methane combustion obtaining 100% conversion at about 480 °C and still maintained high conversion in the presence of water vapor and SO_2.

[090] Accordingly, the present disclosure also includes a supported catalyst comprising a solid catalyst support, and a coating comprising the nanoparticles of the present disclosure.

[091] In an embodiment, the support comprises a bed of alumina, silica, silicon carbide, metal oxide, ceramic, steatite particles, pellets or any combinations thereof. In another embodiment, the support is a monolithic catalyst support, such as a monolithic ceramic support. The ceramic can be any suitable ceramic, the selection of which can be made by a person skilled in the art. In an embodiment, the monolithic ceramic support comprises, consists essentially of or consists of cordierite. In alternative embodiment, the support is a corrugated metal foil. In some embodiments, the support forms a honeycomb structure.

[092] In some embodiments, the coating further comprises a secondary support (carrier). For example, such a coating can be prepared by a method comprising: applying a suspension (e.g. an aqueous suspension) comprising nanoparticles of the present disclosure and a secondary support precursor to the solid support; heating to achieve calcination; and optionally repeating the applying and heating until a coating containing a desired catalyst loading is obtained. In an embodiment, the secondary support comprises alumina. In another embodiment, the secondary support precursor is colloidal alumina.

[093] The catatysts of the present disclosure may be used in catalytic convertors, for example in a catalytic convertor for use within an internal combustion engine, wherein the internal combustion engine may be fueled at least in part by methane. Accordingly, in an

embodiment, the catalyst is present in a catalytic converter. In an embodiment, the catalytic convertor is for a vehicle and the gaseous stream is the exhaust of the vehicle. For example, the vehicle can be any suitable vehicle such as a motorcycle, car, truck or bus. In another embodiment, the vehicle is fueled by natural gas. In an embodiment, the gaseous stream passed over the catalyst is the exhaust from a natural gas fueled vehicle and the catalyst faciliates combustion of methane in the gaseous stream. The natural gas may be compressed natural gas (CNG) or liquefied natural gas (LNG).

[094] In an embodiment, the catalytic convertor is for a stationary power generator. In an embodiment, the catalytic converter is in a stationary power generator and the gaseous stream is the exhaust of the stationary power generator. In another embodiment of the present disclosure, the stationary power generator is fueled by natural gas.

[095] The present disclosure also includes a catalytic convertor comprising a supported catalyst of the present disclosure. In an embodiment, the catalytic convertor is for use with an internal combustion engine. In an embodiment, the internal combustion engine is fueled at least in part by methane. In an embodiment, the catalytic convertor is for a vehicle. The vehicle can be any suitbale vehicle such as a motorcycle, car, truck, or bus. In another embodiment, the vehicle is a natural gas fueled vehicle.

[096] The present disclosure also includes an exhaust system (e.g. a vehicle exhaust system) comprising one or more exhaust conduits and a catalytic convertor of the present disclosure. The present disclosure also includes a stationary power generator comprising a catalytic convertor of the present disclosure. The present disclosure also includes a vehicle comprising a catalytic convertor of the present disclosure.

[097] The following are non-limiting examples of the present disclosure:

EXAMPLES

Example 1: Preparation and characterization of $CoCr_2O_4$ particles

I: Materials and Methods

[098] **(a) General:** Cobalt(II) nitrate hexahydrate (Sigma-Aldrich, $\geqslant$ 98%), chromium(III) nitrate nonahydrate (Fisher Scientific, > 96%), methanol (Sigma-Aldrich, $\geqslant$ 99.8%), benzyl alcohol (Sigma-Aldrich, $\geqslant$ 99%), and other solvents were used without further purification.

[099] **(b) Instrumentation:** Filtrates and final products from the above examples were characterized, *inter alia* by FT-IR spectroscopy, elemental analysis (EA), powder X-ray diffraction (PXRD), thermogravimetric analysis (TGA) and energy dispersive X-ray (EDX) analysis.

[100] Powder X-ray diffraction (PXRD) data were collected with a Bruker D8 Advance X-ray diffractometer using Cu Kα radiation at 40 mA, 40 kV. Fourier transform infrared (FT-IR) spectroscopy was conducted on a PerkinElmer Frontier FT-IR spectrometer. Brunauer–Emmett–Teller (BET) surface areas were measured by N_2 adsorption at 77 K using a Micromeritics Accelerated Surface Area & Porosity (ASAP) 2020 system. High-resolution transmission electron microscopy (HRTEM) images were collected on a FEI Tecnai G2 electron microscope with an accelerating voltage of 200 kV. Scanning electron microscopy (SEM) images were recorded on a Hitachi S-4700 FESEM operating at 5 kV accelerating voltage. Energy-dispersive X-ray (EDX) data were obtained with a Hitachi S2600 Variable Pressure SEM with an X-ray detector. EDX mapping data were collected on a FEI Tecnai Osiris S/TEM at an operating voltage of 200 kV. X-ray photoelectron spectroscopy (XPS) data were obtained using a Leybold Max200 spectrometer with an ion-pumped chamber (1×10^{-9} Torr). The active sites of the catalysts were determined using CO chemisorption with a Micromeritics AutoChem 2920 analyzer. Samples were purged with helium at 373 K for 2 h to remove moisture, and then reduced by H_2 at 773 K. Pulses of CO were then passed over the sample at 323 K and CO adsorption measured with a thermal conductivity detector (TCD).

II: Synthetic Procedures

(a) Solvothermal preparation of $CoCr_2O_4$ nanoparticles in methanol

[101] Cobalt(II) nitrate hexahydrate ($Co(NO_3)_2 \cdot 6H_2O$, 0.5867 g, 2.000 mmol) and chromium(III) nitrate nonahydrate ($Cr(NO_3)_3 \cdot 9H_2O$, 1.614 g, 4.000 mmol) were added to 20 mL methanol and stirred. The mixture was then transferred to a 45 mL Teflon-lined stainless steel autoclave and the sealed reaction vessel was maintained at 180 °C for different lengths of time (1, 8, 24 h). After the reaction was cooled to ambient temperature, the autoclave contents were collected by suction filtration and the dark green product was washed with ethanol for 3 times. Finally, the sample was dried at 100 °C for 2 h and calcined under air at 500 °C for 3 h. Yields are summarised in Table 1.

Table 1

Solvothermal reaction time for $CoCr_2O_4$	Yield after solvothermal reaction (g)	Yield after calcination (g)
Control-1h	0.6171	0.4152
Control-8h	0.6401	0.4228
Control-24h	0.5952	0.4067

(b) Solvothermal preparation of $CoCr_2O_4$ nanoparticles in methanol plus benzyl alcohol

[102] Cobalt(II) nitrate hexahydrate ($Co(NO_3)_2 \cdot 6H_2O$, 0.5867 g, 2.000 mmol) and chromium(III) nitrate nonahydrate ($Cr(NO_3)_3 \cdot 9H_2O$, 1.614 g, 4.000 mmol) were dissolved in 20 mL methanol. Benzyl alcohol (3 mL, 29.00 mmol) was added and the solution was stirred for 1 h. The mixture was then transferred to a 45 mL Teflon-lined stainless steel autoclave. The sealed reaction vessel was maintained at 180 °C for different lengths of time (1, 3, 6, 8, 12, 24 h). After the reaction cooled to ambient conditions, the autoclave contents were collected by suction filtration. The dark green product was washed with ethanol three times, then dried at 100 °C for 2 h and calcined at 500 °C for 3 h. Yields are summarised in Table 2. The catalysts are identified by the solvothermal reaction time used (i.e. 1h, 3h, 6h, 8h, 12h and 24h).

Table 2

Solvothermal reaction time in methanol and benzyl alcohol	Yield after solvothermal reaction (g)	Yield after calcination (g)
1 h	0.6484	0.4196
3 h	0.6856	0.4224
6 h	0.7492	0.4324
8 h	0.7500	0.4466
12 h	0.7544	0.4473
24 h	0.6819	0.4360

(c) Hydrothermal preparation of $CoCr_2O_4$ particles precipitated with NaOH

[103] Cobalt(II) acetate tetrahydrate ($Co(CH_3CO_2)_2 \cdot 4H_2O$, 0.8303 g, 3.333 mmol) and chromium(III) acetate hydrate ($Cr(CH_3CO_2)_3 \cdot H_2O$, 4.022 g, 6.667 mmol) were dissolved in 40 mL deionized water at 70 °C while stirring. A sodium hydroxide solution (prepared by dissolving 1.067 g NaOH in 10 mL H_2O) was added to the metal salt solution dropwise and the mixture continued stirring for 1 h at 70 °C. Afterward, the precipitate was collected by filtration, washed with H_2O and dried in an oven at 100 °C for 8 h. Finally, the product was calcined at 500 °C for 3 h.

(d) Hydrothermal preparation of $CoCr_2O_4$ particles precipitated with NH_4OH

[104] Cobalt(II) nitrate hexahydrate ($Co(NO_3)_2 \cdot 6H_2O$, 0.7276 g, 2.500 mmol) and chromium(III) nitrate nonahydrate ($Cr(NO_3)_3 \cdot 9H_2O$, 2.001 g, 5.000 mmol) were dissolved in 30 mL deionized water. 10 wt % NH_4OH solution (10 mL NH_4OH diluted with 20 mL H_2O) was added to the above metal salt solution dropwise until the pH equaled to 9, then the

mixture was stirred for 1 h. The precipitate was obtained by filtration, washed with H_2O and dried in oven at 100 °C for 8 h. Finally, the product was calcined at 500 °C for 3 h.

(e) Hydrothermal preparation of $CoCr_2O_4$ particles precipitated with an amine

[105] Cobalt(II) nitrate hexahydrate (0.146 g, 0.500 mmol) and chromium(III) nitrate nonahydrate (0.404 g, 1.00 mmol) were dissolved in 20 mL of deionized water. A solution of oleylamine (4 mL, 12 mmol) in 10 mL of ethanol was added to the above solution under vigorous stirring. The mixture was stirred for 30 min under air, and then transferred to a 45 mL Teflon-lined stainless steel autoclave. The sealed reaction vessel was heated to 180 °C for 12 h. After cooling down to room temperature, the precipitate was washed by centrifugation three times with 40 mL ethanol. Then the product was dried at 80 °C for 5 h and calcined at 500 °C for 3 h.

III: Results and Discussion

[106] FT-IR spectroscopy was used to study the reaction mixtures prior to the solvothermal reaction, and the filtrate following the reaction. As shown in FIG. 1, before the solvothermal reaction described above in I(b), peaks due to methanol (broad band at 3318 cm^{-1}, $v_{(C-H)}$) and benzyl alcohol (1019 cm^{-1}, $v_{(C-O)}$; about 1495 cm^{-1}, phenyl ring vibrations; about 3000 cm^{-1} $v_{(C-H)}$)[39] were observed. After solvothermal reaction for 24 h, and removal of the remaining methanol by rotary evaporation, a peak at 1700 cm^{-1} ($v_{(C=O)}$)[40] was present, indicative of the formation of benzaldehyde, in addition to peaks attributed to benzyl alcohol. This suggests a fraction of the benzyl alcohol was oxidized to form benzaldehyde during the solvothermal reaction. Solvothermal reaction of the mixture of methanol and benzyl alcohol under the same conditions without cobalt or chromium salts present did not yield any benzaldehyde, indicating that the metal salts are involved in the oxidation of benzyl alcohol to benzaldehyde.

[107] Precipitate collected from the solvothermal reactions was washed, dried and characterized. PXRD analysis (FIG. 2) indicated that the as-formed product is essentially amorphous. Weak cobalt oxide peaks appear in the PXRD pattern of the sample after one hour of solvothermal reaction. As the solvothermal reaction time is increased, the intensity of these peaks decreased, suggesting that the ratio of Co_3O_4 in the precipitate decreased. FTIR spectra of the product, as shown in FIG. 3 indicate the presence of both benzoate groups and alkoxy groups. Strong bands at 1594 and 1394 cm^{-1} are assigned to asymmetric and symmetric C=O stretching of carboxylate groups, respectively. Peaks at 1068, 1025, and 1177 cm^{-1} are due to C-H phenyl in-plane bending, and a peak at 1495 cm^{-1} is assigned to phenyl stretching modes. Medium strength bands at 2931, 2825 cm^{-1} are assigned to the antisymmetric and symmetric stretching modes of CH_3. The strong band at 1022 cm^{-1} is attributed to C-O stretching. FTIR spectra of the product obtained from solvothermal reaction

in methanol without adding benzyl alcohol, shown in FIG. 4, indicated the presence of formate from strong bands at 1586 and 1355 cm^{-1}. The strong band at 1031 cm^{-1} is attributed to C-O stretching. Medium strength bands at 2935, 2823 cm^{-1} are assigned to the antisymmetric and symmetric stretching modes of CH_3. Elemental ratios in the samples were determined by EDX and EA, these data are summarized in Table 3. Data in parentheses were determined by combustion elemental analysis. While not wishing to be limited by theory, the difference in C analysis likely arises from the fact that XPS profiles a limited depth while combustion analysis gives a bulk analysis. The C analysis from combustion is most accurate for bulk material, whereas XPS is most useful for determining elemental ratios in the samples. Based on the carbon analysis, addition of benzyl alcohol resulted in the precipitate trapping more organic groups (e.g., methoxy and/or benzoate groups). These results were in agreement with TGA results shown in FIG. 5. The $CoCr_2O_4$ product prepared with 24 h of hydrothermal reaction time in methanol plus benzyl alcohol lost more mass than a sample prepared for the same reaction time with no benzyl alcohol present.

Table 3

$CoCr_2O_4$ precursor	Co (wt %)	Cr (wt %)	C (wt %)	O (wt %)	H (wt %)
1 h	9.1	15.9	33.0 (11.2)	42.0	(3.1)
8 h	14.1	25.7	28.9 (11.9)	31.3	(3.7)
24 h	14.2	22.6	30.3 (12.8)	32.9	(3.4)
Control-1h	21.5	40.0	16.4	22.2	
Control-8h	22.3	39.7	16.1	22.0	
Control-24h	22.5	41.5	16.0 (5.0)	21.0	(3.7)

[108] In summary, with the use of methanol and benzyl alcohol, cobalt and chromium alkoxy benzoate composites co-precipitated, yielding a green powder. At the same time, Co^{2+} and Cr^{3+} catalyzed the oxidation of benzyl alcohol to benzaldehyde and benzoate. The benzoate groups may bind with cobalt and chromium ions and coat the surface of precipitates. Furthermore, part of Co^{2+} salts are oxidized to Co_3O_4 at an early stage. Co_3O_4 nanoparticles are reduced back to Co^{2+} and combined with Cr^{3+} to gradually form $CoCr_2O_4$ precursor.

[109] Morphology and structure of the $CoCr_2O_4$ nanoparticles were further investigated by SEM, PXRD, EDX mapping, and high-resolution transmission electron microscopy (HRTEM). Samples were prepared with different solvothermal reaction times (1 - 24 h) in order to explore the growth process of the $CoCr_2O_4$ nanoparticles.

[110] The separated precipitate was subsequently calcined at 500 °C for 3 h, during which time it decomposed to oxide. As shown in FIG. 6, PXRD data shows that the major product matches the standard cochromite $CoCr_2O_4$ (JCPDS 22-1084). There is also a small amount of Co_3O_4 and Cr_2O_3 present at the early stages of the reaction (short solvothermal reaction time). With longer solvothermal treatment, the peaks for Co_3O_4 and Cr_2O_3 decreased in intensity relative to $CoCr_2O_4$, and were completely absent after about 8 hours solvothermal reaction time. An enlarged PXRD pattern is shown in FIG. 7.

[111] In some embodiments, the precipitate and the resulting $CoCr_2O_4$ nanoparticles will be substantially free of Co_3O_4 and Cr_2O_3 and/or substantially free of adhered Co_3O_4 particles with at least about 8 hours to about 24 hours of solvothermal reaction time. As shown in FIG. 8, large $CoCr_2O_4$ particles (500-800 nm) that are decorated with smaller Co_3O_4 nanostructures (<100 nm) initially form. After 1 h solvothermal reaction in methanol plus benzyl alcohol, the Co_3O_4 nanostructures are solid, while at 8 h, they appear to be hollow spheres. As the solvothermal reaction time increases, the number of parasitic nanoparticles decreases and the large $CoCr_2O_4$ particles appeared to have a smoother surface. At 24 h, all of the Co_3O_4 nanostructures are gone and the surface of the $CoCr_2O_4$ nanoparticles is smooth. We believe the alcohol may have a role in controlling the particle size and smoothness of the particle surfaces during formation. The addition of benzyl alcohol may facilitate redox reactions of the transition metal ions, enabling the formation of homogeneous mixed oxide structures. Furthermore, particle size may be controlled, possibly through surface capping with benzoate groups.

[112] PXRD data (FIG. 6) of $CoCr_2O_4$ show broadening of the diffraction peaks arising from small domain sizes. The Scherrer equation was applied to calculate particle sizes of the crystalline $CoCr_2O_4$ components, as summarized in Table 4. It is evident that the nanodomains (about 6-10 nm) of $CoCr_2O_4$ grow larger with increasing solvothermal reaction times. Owing to overlap between the peaks due to Co_3O_4 and Cr_2O_3 and other phases, as well as the effects of background noise, it was not possible to estimate the particle sizes of Co_3O_4 and Cr_2O_3, through broadening of the peaks suggest they are also small.

Table 4

Sample	Particle size determined from (220) (nm)	Particle size determined from (311) (nm)
6 h	7.0	6.1
8 h	8.6	7.2
12 h	9.0	7.5
24 h	10.4	8.4

[113] Samples prepared with solvothermal reaction times of 1, 3, 8, and 24 h were selected for characterization by EDX mapping. Using this technique, the parasitic nanostructures are assigned to Co_3O_4 (FIG. 9). After 1 h solvothermal reaction, the Co_3O_4 nanostructures are solid, while after 8 h, they appear to be hollow spheres (arrow in FIG. 9). FIG. 10 shows an enlarged SEM image, where several nanostructures, as indicated by arrows, are split open revealing their hollow structures. Due to the finite crystal size of hollow nanostructured Co_3O_4 and its diminishing quantity with increasing reaction time, the peak for Co_3O_4 in the PXRD is not present after 8 h. The large $CoCr_2O_4$ nanoparticles contain a small amount of crystalline Cr_2O_3 (particle size is about 200 nm, measured according to EDX mapping) after one hour of solvothermal treatment. After three hours, the crystal size of Cr_2O_3 decreased (to about 100 nm) and these nanocrystals are distributed more evenly on the surface of the $CoCr_2O_4$. Co and Cr are homogeneously mixed in the large nanoparticles prepared with longer solvothermal reaction times (8 h, 24 h). These results were in agreement with the PXRD data.

[114] In contrast, in the preparation conducted without adding benzyl alcohol, after one hour of solvothermal treatment, (Control-1h), separate Co_3O_4 and Cr_2O_3 phases are apparent (FIG. 11). After 24 h reaction time, the solid Co_3O_4 can still be observed (Control-24h) and the particle size of $CoCr_2O_4$ is not uniform.

[115] To further characterize the products, a detailed HRTEM study was undertaken. The nanoparticles formed from the aggregation of nanocrystals with sizes around 10 nm (FIG. 12) in diameter, which agrees with the domain size calculated from the PXRD data by the Scherrer equation. Lattice fringes with 0.48 nm spacing were observed and correspond to the (111) planes of $CoCr_2O_4$. The lattice spacing for the parasitic nanostructures was 0.40 nm, assigned to the (200) planes of Co_3O_4.

[116] Nitrogen adsorption-desorption analysis was used to determine the surface area and pore size distribution of the solvothermal products at each stage of the reaction, as shown in Table 5. Brunauer-Emmett-Teller (BET) analysis gave surface area at 77 K of at least 100 $m^2\ g^{-1}$ with a pore size of about 6 nm. There were no significant differences between the samples prepared with different solvothermal reaction times: 1-24 hours in methanol plus benzyl alcohol as well as in methanol alone for 24 hours (Control – 24h). As will be discussed below, the $CoCr_2O_4$ particles show superior catalytic activity, in part due to their smooth surface and large surface area.

Table 5

Sample	Surface area (m^2 g^{-1})	Pore size (nm)	Pore volume (cm^3 g^{-1})
1 h	102	6.8	0.17
3 h	106	6.4	0.15
6 h	108	6.2	0.16
8 h	101	6.0	0.15
12 h	108	6.4	0.17
24 h	114	6.2	0.18
Control-24h	103	6.0	0.16

[117] The sample prepared by the hydrothermal method using oleylamine as precipitation agent was also characterized by TEM spectroscopy. The shape of these nanocrystal products were irregular and their particle size was from 20 to 50 nm. The small particle size may, for example, result in sintering and aggregation during catalysis reactions, which lead to deactivation of catalysts and poor catalytic stability.

[118] XPS spectra of $CoCr_2O_4$ were used to assess the surface composition of the catalysts prepared with different solvothermal reaction times. In the O 1s spectra (FIG. 13) the peak at 530.7 eV is assigned to surface lattice oxygen (O_{latt}), while the peak at 533.2 eV is characteristic of adsorbed oxygen (O_{ads}), and the peak at 533.23 eV is due to carbonate or adsorbed water species.[41] The sample prepared with the addition of benzyl alcohol has significant carbonate coverage on the surface, which may increase the catalyst's resistance to poisoning by impurities in the gas stream. The peaks at 578.7 and 576.9 eV are assigned to C^{r6+} and Cr^{3+}, respectively.[42] It was proposed in previous studies that a large amount of adsorbed oxygen species benefits the adsorption and activation of reactants, and a higher surface ratio of Cr^{6+}/Cr^{3+} improves the low temperature reducibility.[43] These data for our samples are summarized in Table 6. The ratio of Cr^{6+}/Cr^{3+} for the sample prepared with benzyl alcohol is higher than for the control sample (Control-24 h). The control sample contained more lattice O and less adsorbed O on the surface. Based on the surface elemental ratio (Co/Cr in Table 6), there is more cobalt detected on the surface for the control sample. Cobalt oxide is more active but less stable than chromium oxide,[29] so the control sample may be less stable than the catalysts prepared with benzyl alcohol. From the XPS data, it appears that the addition of benzyl alcohol changes the surface elemental ratio and surface coverage of the catalysts and this may affect their activity and stability.

Table 6

$CoCr_2O_4$	Cr^{6+}/Cr_{total}	O_{latt}/O_{ads}	Co/Cr
1 h	0.32	0.24	0.14
3 h	0.37	0.33	0.12
6 h	0.36	0.93	0.14
Control-24h	0.22	2.5	0.34

Example 2: Catalytic performance of $CoCr_2O_4$ particles

I: Materials and Methods

[119] **(a) Evaluation of catalytic performance:** Catalytic performance of products was evaluated by temperature-programmed CH_4 oxidation (TPO) in a gas mixture containing 1000 ppmv CH_4, 10% (V/V) O_2, and Ar, He balance at a flow rate of 300 mL/min. The catalyst (0.1000 g) was mixed with 2.5000 g SiC and then transferred into a stainless steel fixed-bed microreactor. The reactor was heated from room temperature to 600 °C at a rate of 5 °C min^{-1} while the composition of emitted gas was analyzed by a VG ProLab quadrupole mass spectrometer (QMS; ThermoFisher Scientific). Conversion was calculated by determination of the yield of CO_2 and total carbon balance. Stability studies of the catalysts were conducted at 500 °C with 10% H_2O and 5 ppm SO_2 added to the dry feed gas prior to the preheater.

II: Results and Discussion

[120] The TPO experiments resulted in a light off-curve, giving the conversion as a function of temperature. The light-off curves measured for the $CoCr_2O_4$ catalysts are shown in FIG. 14 (all catalysts were tested after calcination at 500 °C). The overall reactivities are as follows: 1 h ≈ 3 h ≈ 6 h ≈ 8 h > 12 h > 24 h. $CoCr_2O_4$ catalysts prepared with solvothermal reaction times less than 24 h all achieved 100% conversion below 500 °C.

[121] The catalytic performances of $CoCr_2O_4$ catalysts prepared by different methods were compared (FIG. 15), and the activities for the catalysts were as follows: $CoCr_2O_{4\ 8h}$ (methanol and benzyl alcohol) ≈ $CoCr_2O_{4\ Control\text{-}24h}$ (methanol alone) > Co_3O_4 > $CoCr_2O_{4\ NH4OH}$ precipitate > Cr_2O_3 > $CoCr_2O_{4\ NaOH}$. Apparent activation energies (E_a) were calculated based on Arrhenius plots for methane oxidation as shown in FIG. 16 and in Table 7. Co_3O_4 had the lowest activation energy (E_a = 46.5 kJ/mol), and Cr_2O_3 had the highest among the tested catalysts. Addition of cobalt into chromium oxide to give $CoCr_2O_4$ catalysts lowers the methane activation barrier compared with pure Cr_2O_3. $CoCr_2O_{4\ 8h}$ and $CoCr_2O_{4\ Control\text{-}24h}$ demonstrated the same excellent activities but different activation energies. $CoCr_2O_4$

precipitated by NaOH had a lower activation energy but was less active than Cr_2O_3. Therefore, activation energy is not the only effect on catalytic activity. CO chemisorption was used to calculate the number of active sites for the catalysts, and turn-over frequency (TOF) was calculated based on the number of active sites. The results are also summarized in Table 7. The catalysts with lower E_a have higher TOF. This indicates that the catalysts with lower activation energy are more effective at methane combustion on a per site basis. Catalysts with more effective active sites but without enough exposed sites may not exhibit the best catalytic performance. Although Co_3O_4 is more active per site, it has fewer active sites exposed and, as a consequence, it is not as active as $CoCr_2O_{4\ 8h}$ or $CoCr_2O_{4\ Control\text{-}24h}$. Above all, both the efficiency and the number of active sites determine the final catalytic performance.

Table 7

Catalysts	Active sites (μmol/g)	E_a (kJ/mol)	TOF (s^{-1}) at 330 °C	$T_{50\%}$ (°C)
$CoCr_2O_{4\ 8h}$	27.3	71.5	0.0090	396
$CoCr_2O_{4\ Control\text{-}24h}$	23.1	58.6	0.0101	396
$CoCr_2O_{4\ NH4OH}$	8.8	76.8	0.0077	484
$CoCr_2O_{4\ NaOH}$	7.8	79.6	0.0041	537
Co_3O_4	8.9	46.9	0.0348	415
Cr_2O_3	22.0	108.6	0.0010	510

[122] The stability of the catalysts prepared as described above in Example 1 was probed using the addition of 10% water and 5 ppm SO_2 to the gas feed at 500 °C, as summarized in FIG. 17 and Table 8. The activity for $CoCr_2O_4$ prepared with benzyl alcohol present and a 24 h solvothermal reaction time dropped immediately from 98% to 80% activity. After about 12 h treatment with this gas mixture (at 500 °C), the activity remained stable at about 78%. The activity for $CoCr_2O_4$ prepared with benzyl alcohol present and 8 h solvothermal reaction time dropped to 92% in the presence of SO_2 and water, then the activity gradually decreased to 88% and remained relatively stable at this value. The catalysts prepared with only 1 h solvothermal treatment showed slightly poorer stability. After injection of SO_2 and water, their activity continuously decreased from 100% to about 82%, and the activity returned to 94% after removing SO_2 and water. Among the samples studied, $CoCr_2O_4$ prepared with benzyl alcohol and 8 h solvothermal treatment exhibited the best stability. The conversion for control catalysts (prepared in methanol alone) decreased more in the presence of water and SO_2.

Table 8

$CoCr_2O_4$	Conversion drops at the beginning of H_2O and SO_2 injection	Conversion in the presence of SO_2 and H_2O within 13 h	Decreased conversion in total
24 h	98-80% (Δ = 18%)	80-78% (Δ = 2%)	20%
Control-24h	100-90% (Δ = 10%)	90-84% (Δ = 6%)	16%
8 h	100-92% (Δ = 8%)	92-88% (Δ = 4%)	12%
Control-8h	95-75% (Δ = 20%)	75-66% (Δ = 8%)	28%
1 h	-	99-85% (Δ = 14%)	14%
Control-1h	96-82% (Δ = 14%)	82-69% (Δ = 13%)	28%

[123] The catalytic activity and stability measurements for the catalysts prepared without addition of benzyl alcohol during the solvothermal reaction are shown in FIGS. 18 and 19. The control catalysts prepared with a longer solvothermal treatment time showed lower methane conversion temperatures, which is opposite to the trend for $CoCr_2O_4$ prepared with benzyl alcohol. Furthermore, the light off curve for Control-24h is similar to that for $CoCr_2O_4$ prepared in 8 h. Control-1h and Control-8h show nearly the same catalytic performance, but they are less active than all the catalysts prepared with benzyl alcohol. As for the stability, the conversion for control catalysts decreased more in the presence of water and SO_2, as summarized in Table 9. Thus, the catalysts prepared using benzyl alcohol showed greater stability compared with the control catalysts, which is in agreement with the conclusions drawn from the XPS data.

[124] To better understand the catalytic mechanism, the reducibility and chemical states of the catalysts were investigated. The reducibility was measured by H_2-TPR (temperature-programmed reduction). The H_2-TPR profile of Co_3O_4 shows two reduction peaks (FIG. 20), which indicated reduction of Co^{3+} to Co^{2+} and Co^{2+} to Co^0. Cr_2O_3 exhibits a peak at about 212 °C that is ascribed to the reduction of Cr^{6+} to Cr^{3+}. However, the initial reduction temperatures for $CoCr_2O_4$ samples, even those prepared by different methods, are lower than for Co_3O_4 or Cr_2O_3. According to a previous study,[44] due to the equilibrium $Cr^{6+} + 3Co^{2+} \leftrightarrow Cr^{3+} + 3Co^{3+}$, the reducibility of Cr^{6+} and Co^{3+} may be further improved. The lower reduction temperature may indicate higher oxygen mobility. Therefore, the lower reduction temperature is attributed to the synergistic effect of Cr^{6+} and Co^{3+}, and surface oxygen species. Catalysts consuming more H_2 at lower temperature indicates higher reducibility. As summarized in Table 9, the relative reducibility of the different catalysts is $CoCr_2O_{4\ Control\text{-}24h} > CoCr_2O_{4\ 8h} > CoCr_2O_{4\ NH4OH} > CoCr_2O_{4\ NaOH}$. The H_2-TPR for $CoCr_2O_4$ precipitated by NH_4OH or NaOH shows peaks from 250 to 400 °C. For $CoCr_2O_4$ prepared by the solvothermal method, the peaks from 250 to 400 °C are very

weak. This indicates that the combination of Co and Cr in $CoCr_2O_4$ prepared by the solvothermal method is better than the co-precipitation method. Above all, the spinel $CoCr_2O_4$ catalysts prepared by the solvothermal method improved the interaction between Co and Cr elements, which further enhanced the reducibility at low temperature.

Table 9

$CoCr_2O_4$	H_2 consumption T<250 °C (mmol/g (°C))	TOF (s^{-1})
$CoCr_2O_{4\ 8h}$	0.39 (192)	0.0090
$CoCr_2O_{4\ Control\text{-}24h}$	0.42 (207)	0.0101
$CoCr_2O_{4\ NH4OH}$	0.16 (180)	0.0077
$CoCr_2O_{4\ NaOH}$	0.12 (171)	0.0041
Co_3O_4	0.62 (233)	0.0348
Cr_2O_3	0.18 (212)	0.0010

[125] Previous reports indicated that oxidative reactions over Co_3O_4 follow a redox cycle of $Co^{3+} \leftrightarrow Co^{2+}$,[45] and the rate-determining step of C-H dissociation accompanies metal oxide reduction.[46] Therefore, easily-reduced catalyst oxides contribute to the initial highly activity for low temperature methane oxidation. As shown in FIG. 20, for pure Co_3O_4, the reduction of Co^{3+} consumed a lot of H_2 at lower temperature, which indicates that the Co^{3+} can be easily reduced. Thus, Co^{3+} ions are considered to play an important role during methane oxidation.[28] However, the easy reduction may lead to a higher mobility of Co ions which result in agglomeration and poor stability. This may, for example, explain the phenomenon that after long term stability tests, Co_3O_4 crystals appear on the surface and Cr_2O_3 is sintered within the $CoCr_2O_4$ catalysts. The synergistic effect of chromium and cobalt in the spinel structure improves the reducibility and stability of the catalysts. The presence of Cr^{6+} may cause the $CoCr_2O_4$ to have more defects exposed on the surface of catalysts.[28] This is expected to improve the oxygen chemisorption and contribute to catalytic methane combustion. For example, the catalysts with better reducibility exhibit higher TOF for low temperature methane combustion, which is in agreement with the proposed mechanism.

[126] After dissociation of the C-H bonds, oxygen mobility contributes to further oxidizing intermediates to eventually yield CO_2 and H_2O. Oxygen mobility is assessed herein using O_2-TPR. $CoCr_2O_4$ catalysts exhibit lower O_2 desorption temperature compared with pure metal oxide (FIG. 21). This indicates improved oxygen mobility after incorporation of Cr into the spinel cobalt oxide structure which is in agreement with the H_2-TPR results. The poor oxygen mobility for Co_3O_4 explains why there is lower methane oxidation activity compared to $CoCr_2O_4$, after initiation of the reaction.

[127] XPS spectra were collected to investigate the surface chemical state and composition. Given the large differences in catalytic activity for pure Co_3O_4 and Cr_2O_3 catalysts, the surface Co/Cr ratio may play an important role in catalysis. Also, the presence of easily reduced Co^{3+}, Cr^{6+} and adsorbed oxygen improves the catalytic methane oxidation and Co_3O_4 exhibits the lowest activation energy, while Cr_2O_3 shows the highest activation energy. For $CoCr_2O_4$ catalysts, Control-24h has more exposed Co^{3+} compared with 8h and NH_4OH samples, so it has lower E_a (Table 10). $CoCr_2O_{4\ NaOH}$ shows a higher Co ratio on the surface but much higher lattice O ratio, therefore, it still has higher E_a than Control-24h. Combined with the number of active sites, we observe that the catalysts synthesized with the same method, where the surface has more Co exposed, has a lower number of active sites. For example, for the $CoCr_2O_4$ 8h catalyst, the synergistic effect of Cr^{6+} and Co^{3+} improved the reducibility, and gives the appropriate surface Co/Cr ratio which can expose more active sites contributes to the final catalytic conversion.

Table 10

$CoCr_2O_4$	Co^{3+}/Co_{total}	Cr^{6+}/Cr_{total}	O_{latt}/O_{ads}	Co/Cr
$CoCr_2O_{4\ 8h}$	0.32	0.37	0.33	0.12
$CoCr_2O_{4\ Control\text{-}24h}$	0.68	0.22	2.5	0.34
$CoCr_2O_{4\ NH4OH}$	0.41	0.34	0.51	0.10
$CoCr_2O_{4\ NaOH}$	0.66	0.26	18	0.48
Co_3O_4	0.89	-	0.64	-
Cr_2O_3	-	0.29	2.5	-

[128] The calcined $CoCr_2O_4$ catalyst prepared with methanol plus benzyl alcohol and an 8 h solvothermal treatment as described hereinabove in Example 1 was heated to 500 °C in 20 min under a flowing MOX gas mixture (1000 ppm CH_4, 10% O_2), then 10% water and 5 ppm SO_2 were injected into the gas feed. After 12-25 h, water and SO_2 were stopped and the reaction continued for another 2 h to probe reversibility. For the first run, the conversion decreased about 5% in the presence of water and SO_2 over 12 h (see Table 11 and FIG. 22). The observed loss of activity under water and SO_2 became smaller after several cycles. After seven runs, the conversion was stable at 78% in wet conditions with SO_2 present, and 93% in dry conditions. There were no significant differences for the final three runs. The $CoCr_2O_4$ catalyst therefore shows excellent stability and durability for low temperature methane combustion in the presence of water and SO_2.

Table 11

$CoCr_2O_4$ 8h	Time (h)	Conversion in the presence of H_2O and SO_2 (%)	Reversibility (%)
1st run	13	96-91	100-100
2nd run	15	92-88	100-99
3rd run	13.5	87-86	97-97
4th run	12.5	87-85	96-96
5th run	14	85-83	95-95
6th run	16.5	84-81	96-95
7th run	18	82-80	94-94
8th run	23	80-78	93-93
9th run	24.5	79-77	92-92
10th run	17	78-78	93-93

[129] To investigate the reasons underlying the catalyst deactivation, the spent catalysts were analyzed by TEM, EDX and PXRD. After the durability test, the aggregation of large chromium oxide particles was observed (FIG. 23). Moreover, regular cobalt oxide nanoparticles (about 100 nm) were distributed on the surface of the nanospheres (FIG. 24). These results are in agreement with the PXRD data (FIG. 25). As well, new diffraction peaks appeared in the $CoCr_2O_4$ 8 h sample after the durability test, assigned to Cr_2O_3. Particle sizes (see Table 12) for the used catalysts are all larger than the fresh ones, and the sintering of the nanoparticles may be responsible for the deactivation of catalysts. No sulfur was detected by XPS and EDX in the catalysts after SO_2 treatment, demonstrating that no sulfate or sulfide compounds form that bind to the surface and poison the catalyst, indicating that the catalysts display good tolerance to sulfur compounds.

Table 12

Sample	Particle size from (220) (nm)	Particle size from (311) (nm)
8h fresh	8.6	7.2
8h used	9.4	8.6
8h long used	14.7	11.8
24h fresh	10.4	8.4
24h used	10.6	8.7
Control-24h fresh	7.2	6.3
Control-24h used	7.5	6.7

Example 3: Catalysis with a coated monolith

I: Materials and Methods

[130] Preparation of the coated monolith: Cordierite monolithic substrates (400 cpsi) were used as support. A catalyst suspension was prepared by mixing the calcined $CoCr_2O_4$ $_{8h}$ catalysts and colloidal alumina solution. Typically, 3.3 mL colloidal alumina solution, 2.0 g $CoCr_2O_4$ 8h catalysts were added to 6.7 mL water under stirring to obtain the suspension. The monolith (about 0.35 g) was dipped into above suspension for 5 min. Then the monolith was removed, and the excess solvent was removed by shaking the monolith and blowing with compressed air. After that the monolith was placed in front of a heat gun (about 300 °C) for about 10 min to achieve calcination. Then the monolith was blown with compressed air again to remove any loose coating. The dipping and quick calcining steps were repeated to obtain a 0.10 g coating. The monolith was calcined in a furnace at 500 °C for 7 h. Finally, the above steps were repeated to get another 0.10 g coating following calcination under the same conditions to obtain a total catalyst loading of 0.20 g.

II: Results and Discussion

[131] Methane combustion was investigated for the coated monolith using the procedure described above. As shown in FIG. 26, the coated monolith exhibited very good catalytic activity obtaining 100% conversion at about 480 °C. When 10% H_2O and 5 ppm SO_2 were injected to the dry gas feed at the beginning and removed after 10 to 18 hours, the coated monolith still maintained high conversion which was stable at 88% after 4 cycles (about 50 h).

[132] The above described embodiments are intended to be illustrative only and in no way limiting. The described embodiments are susceptible to many modifications of form, arrangement of parts, details, and order of operation that would be apparent to the skilled reader. The invention is intended to encompass all such modification within its scope, as defined by the following claims.

[133] All publications, patents and patent applications are herein incorporated by reference in their entirety to the same extent as if each individual publication, patent or patent application was specifically and individually indicated to be incorporated by reference in its entirety. Where a term in the present application is found to be defined differently in a document incorporated herein by reference, the definition provided herein is to serve as the definition for the term.

References

[134] Citation of any publication or patent document herein is not an admission that the reference is prior art to the present invention.

1. Maggio, G.; Cacciola, G., When will oil, natural gas, and coal peak? *Fuel* **2012,** *98*, 111-123.
2. Choudhary, T. V.; Banerjee, S.; Choudhary, V. R., Catalysts for combustion of methane and lower alkanes. *Appl. Catal., A* **2002,** *234* (1), 1-23.
3. Ciuparu, D.; Lyubovsky, M. R.; Altman, E.; Pfefferle, L. D.; Datye, A., Catalytic Combustion of Methane Over Palladium- based Catalysts. *Catal. Rev. Sci. Eng.* **2002,** *44* (4), 593-649.
4. Jiang, X.; Mira, D.; Cluff, D. L., The combustion mitigation of methane as a non-CO_2 greenhouse gas. *Prog. Energy Combust. Sci.* **2018,** *66*, 176-199.
5. Gélin, P.; Primet, M., Complete oxidation of methane at low temperature over noble metal based catalysts: a review. *Appl. Catal., B* **2002,** *39* (1), 1-37.
6. Regulation (EC) No. 595/2009; Annex I.
7. Honkanen, M.; Kärkkäinen, M.; Viitanen, V.; Jiang, H.; Kallinen, K.; Huuhtanen, M.; Vippola, M.; Lahtinen, J.; Keiski, R.; Lepistö, T., Structural Characteristics of Natural-Gas-Vehicle-Aged Oxidation Catalyst. *Top. Catal.* **2013,** *56* (9), 576-585.
8. Chen, J.; Arandiyan, H.; Gao, X.; Li, J., Recent Advances in Catalysts for Methane Combustion. *Catal. Surv. Asia* **2015,** *19* (3), 140-171.
9. Cargnello, M.; Jaén, J. J. D.; Garrido, J. C. H.; Bakhmutsky, K.; Montini, T.; Gámez, J. J. C.; Gorte, R. J.; Fornasiero, P., Exceptional Activity for Methane Combustion over Modular $Pd@CeO_2$ Subunits on Functionalized Al_2O_3. *Science* **2012,** *337* (6095), 713-717.
10. Lou, Y.; Ma, J.; Hu, W. D.; Dai, Q. G.; Wang, L.; Zhan, W. C.; Guo, Y. L.; Cao, X. M.; Guo, Y.; Hu, P.; Lu, G. Z., Low-Temperature Methane Combustion over Pd/H-ZSM-5: Active Pd Sites with Specific Electronic Properties Modulated by Acidic Sites of H-ZSM-5. *ACS Catal.* **2016,** *6* (12), 8127-8139.
11. Willis, J. J.; Goodman, E. D.; Wu, L.; Riscoe, A. R.; Martins, P.; Tassone, C. J.; Cargnello, M., Systematic Identification of Promoters for Methane Oxidation Catalysts Using Size- and Composition-Controlled Pd-Based Bimetallic Nanocrystals. *J. Am. Chem. Soc.* **2017,** *139* (34), 11989-11997.
12. Gholami, R., Deactivation of Pd Catalysts by Water during Low Temperature Methane Oxidation Relevant to Natural Gas Vehicle Converters. *Catalysts* **2015,** *5* (2), 561-594.
13. Burch, R.; Urbano, F. J.; Loader, P. K., Methane combustion over palladium catalysts: The effect of carbon dioxide and water on activity. *Appl. Catal., A* **1995,** *123* (1), 173-184.
14. Monai, M.; Montini, T.; Melchionna, M.; Duchoň, T.; Kúš, P.; Chen, C.; Tsud, N.; Nasi, L.; Prince, K. C.; Veltruská, K.; Matolín, V.; Khader, M. M.; Gorte, R. J.; Fornasiero, P., The effect of sulfur dioxide on the activity of hierarchical Pd-based catalysts in methane combustion. *Appl. Catal., B* **2017,** *202*, 72-83.

15. Sadokhina, N.; Smedler, G.; Nylén, U.; Olofsson, M.; Olsson, L., Deceleration of SO_2 poisoning on $PtPd/Al_2O_3$ catalyst during complete methane oxidation. *Appl. Catal., B* **2018,** *236*, 384-395.

16. Yashnik, S. A.; Chesalov, Y. A.; Ishchenko, A. V.; Kaichev, V. V.; Ismagilov, Z. R., Effect of Pt addition on sulfur dioxide and water vapor tolerance of Pd-Mn-hexaaluminate catalysts for high-temperature oxidation of methane. *Appl. Catal., B* **2017,** *204*, 89-106.

17. Wang, Z.; Deng, J.; Liu, Y.; Yang, H.; Xie, S.; Wu, Z.; Dai, H., Three-dimensionally ordered macroporous $CoCr_2O_4$-supported Au–Pd alloy nanoparticles: Highly active catalysts for methane combustion. *Catal. Today* **2017,** *281*, 467-476.

18. Wu, Z.; Deng, J.; Liu, Y.; Xie, S.; Jiang, Y.; Zhao, X.; Yang, J.; Arandiyan, H.; Guo, G.; Dai, H., Three-dimensionally ordered mesoporous Co_3O_4-supported Au–Pd alloy nanoparticles: High-performance catalysts for methane combustion. *J. Catal.* **2015,** *332*, 13-24.

19. Goodman, E. D.; Dai, S.; Yang, A.-C.; Wrasman, C. J.; Gallo, A.; Bare, S. R.; Hoffman, A. S.; Jaramillo, T. F.; Graham, G. W.; Pan, X.; Cargnello, M., Uniform Pt/Pd Bimetallic Nanocrystals Demonstrate Platinum Effect on Palladium Methane Combustion Activity and Stability. *ACS Catal.* **2017,** *7* (7), 4372-4380.

20. Zhao, X.; Liu, Y.; Deng, J.; Xu, P.; Yang, J.; Zhang, K.; Han, Z.; Dai, H., Mesoporous Pd_xPt alloys: High-performance catalysts for methane combustion. *Mol. Catal.* **2017,** *442*, 191-201.

21. Shen, J.; Hayes, R. E.; Wu, X. X.; Semagina, N., 100 degrees Temperature Reduction of Wet Methane Combustion: Highly Active $Pd\text{-}Ni/Al_2O_3$ Catalyst versus $Pd/NiAl_2O_4$. *ACS Catal.* **2015,** *5* (5), 2916-2920.

22. Toso, A.; Colussi, S.; Padigapaty, S.; de Leitenburg, C.; Trovarelli, A., High stability and activity of solution combustion synthesized Pd-based catalysts for methane combustion in presence of water. *Appl. Catal., B* **2018,** *230*, 237-245.

23. Li, D.; Li, K.; Xu, R.; Wang, H.; Tian, D.; Wei, Y.; Zhu, X.; Zeng, C.; Zeng, L., $Ce_{1-x}Fe_xO_{2-\delta}$ catalysts for catalytic methane combustion: Role of oxygen vacancy and structural dependence. *Catal. Today* **2018,** *318*, 73-75.

24. Wang, H.; Chen, C.; Zhang, Y.; Peng, L.; Ma, S.; Yang, T.; Guo, H.; Zhang, Z.; Su, D. S.; Zhang, J., In situ oxidation of carbon-encapsulated cobalt nanocapsules creates highly active cobalt oxide catalysts for hydrocarbon combustion. *Nat. Commun.* **2015,** *6*, 7181.

25. Zhao, H. Y.; Li, D.; Bui, P.; Oyama, S. T., Hydrodeoxygenation of guaiacol as model compound for pyrolysis oil on transition metal phosphide hydroprocessing catalysts. *Appl. Catal., A* **2011,** *391* (1), 305-310.

26. Hu, W. D.; Lan, J. G.; Guo, Y.; Cao, X. M.; Hu, P., Origin of Efficient Catalytic Combustion of Methane over Co_3O_4 (110): Active Low-Coordination Lattice Oxygen and Cooperation of Multiple Active Sites. *ACS Catal.* **2016,** *6* (8), 5508-5519.

27. Hu, L. H.; Peng, Q.; Li, Y. D., Selective Synthesis of Co_3O_4 Nanocrystal with Different Shape and Crystal Plane Effect on Catalytic Property for Methane Combustion. *J. Am. Chem. Soc.* **2008,** *130* (48), 16136-16137.

28. Sun, Y. N.; Liu, J. W.; Song, J. J.; Huang, S. S.; Yang, N. T.; Zhang, J.; Sun, Y. H.; Zhu, Y., Exploring the Effect of Co_3O_4 Nanocatalysts with Different Dimensional Architectures on Methane Combustion. *Chemcatchem* **2016,** *8* (3), 540-545.

29. Ordóñez, S.; Paredes, J. R.; Díez, F. V., Sulphur poisoning of transition metal oxides used as catalysts for methane combustion. *Appl. Catal., A* **2008,** *341* (1), 174-180.

30. Hu, J.; Zhao, W.; Hu, R.; Chang, G.; Li, C.; Wang, L., Catalytic activity of spinel oxides $MgCr_2O_4$ and $CoCr_2O_4$ for methane combustion. *Mater. Res. Bull.* **2014,** *57*, 268-273.

31. Chen, J.; Zhang, X.; Arandiyan, H.; Peng, Y.; Chang, H.; Li, J., Low temperature complete combustion of methane over cobalt chromium oxides catalysts. *Catal. Today* **2013**, 201, 12-18.

32. Niederberger, M.; Bartl, M. H.; Stucky, G. D., Benzyl Alcohol and Transition Metal Chlorides as a Versatile Reaction System for the Nonaqueous and Low-Temperature Synthesis of Cystalline Nano-Objects with Controlled Dimensionality. *J. Am. Chem. Soc.* **2002,** *124*, 13642-13643.

33. Hu, J.; Zhu, K.; Chen, L.; Yang, H.; Li, Z., Suchopar, A., Richards, R., Preparation and Surface Activity of Single-Crystalline NiO(111) Nanosheets with Hexagonal Holes: A Semiconductor Nanospanner. *J. Adv. Mater.* **2008**, *20*, 267-271.

34. Chen, L.; Hu, J.; Richards, R.; Prikhodko, S.; Kodambaka, S., Synthesis and surface activity of single-crystalline Co_3O_4 (111) holey nanosheets. *Nanoscale* **2010**, *2*, 1657-1660.

35. Wei, R.; Zhou, X.; Zhou, T.; Hu, J.; Ho., J. C., Co_3O_4 Nanosheets with In-Plane Pores and Highly Active {112} Exposed Facets for High Performance Lithium Storage. *J. Phys. Chem. C* **2017**, *121*, 19002-19009.

36. Gomathi, A.; Vickers, S. M.; Gholami, R.; Alyani, M.; Man, R. W. Y.; MacLachlan, M. J.; Smith, K. J.; Wolf, M. O. , Nanostructured Materials Prepared by Surface-Assisted Reduction: New Catalysts for Methane Oxidation. *ACS Appl. Mater. Interfaces* **2015**, *7* (34), 19268-19273.

37. WO 2001/034517.

38. Dai, Y.; Kumar, V. P.; Zhu, C.; Wang, H.; Smith, K. J.; Wolf, M. O.; MacLachlan, M. J., Bowtie - Shaped $NiCo_2O_4$ Catalysts for Low-Temperature Methane Combustion. *Adv. Funct. Mater*. **2019**, *29*,1807519.

39. Higashimoto, S.; Kitao, N.; Yoshida, N.; Sakura, T.; Azuma, M.; Ohue, H.; Sakata, Y., Selective photocatalytic oxidation of benzyl alcohol and its derivatives into corresponding aldehydes by molecular oxygen on titanium dioxide under visible light irradiation. *J. Catal.* **2009**, *266* (2), 279-285.

40. Keresszegi, C.; Ferri, D.; Mallat, T.; Baiker, A., Unraveling the Surface Reactions during Liquid-Phase Oxidation of Benzyl Alcohol on Pd/Al_2O_3: an in Situ ATR−IR Study. *J. Phys. Chem. B* **2005**, *109* (2), 958-967.

41. M. Al-Manum, X. T. Su, H. M. Zhang, H. J. Yin, P. R. Liu, H. G. Yang, D. Wang, Z. Y. Tang, Y. Wang and H. J. Zhao, *Small*, 2016, **12**, 2866.

42. Y. Wang, A.-P. Jia, M.-F. Luo and J.-Q. Lu, *Appl. Catal., B*, 2015, **165**, 477.

43. T. T. Zhang, J. D. Song, J. X. Chen, A. P. Jia, M. F. Luo and J. Q. Lu, *Appl. Surf. Sci.*, 2017, **425**, 1074.

44. C. Liu, H. Xian, Z. Jiang, L. H. Wang, J. Zhang, L. R. Zheng, Y.S. Tan and X. G. Li, *Appl. Catal., B*, 2015, **176**, 542.

45. J. Janson, A. E. C. Palmqvist, E. Fridell, M. Skoglundh, L. Österlund, P. Thormählen and V. Langer, *J. Catal.*, 2002, **211**, 387.

46. Y. Mahara, K. Murata, K. Ueda, J. Ohyama, K. Kato and A. Satsuma, *ChemCatChem*, 2018, **10**, 3384.

CLAIMS:

1. A method of preparing $CoCr_2O_4$ nanoparticles, the method comprising:

heating a solution of a cobalt (II) compound and a chromium (III) compound in an alcohol to form a precipitate;

separating the precipitate from the solution; and

calcining the precipitate to form the $CoCr_2O_4$ nanoparticles.

2. The method of claim 1, wherein the alcohol comprises a C_{1-7}alcohol or mixture thereof.

3. The method of claim 2, wherein the C_{1-7}alcohol or mixture thereof is methanol.

4. The method of any one of claims 1 to 3, wherein the alcohol comprises an alcohol that is a reducing agent and a structure-directing agent.

5. The method of claim 4, wherein the alcohol that is a reducing agent and a structure-directing agent is an aromatic alcohol.

6. The method of claim 5, wherein the alcohol that is a reducing agent and a structure-directing agent is benzyl alcohol.

7. The method of claim 1, wherein the alcohol is a mixture of methanol and benzyl alcohol.

8. The method of any one of claims 1 to 7, wherein the heating of the solution is carried out at a pressure greater than ambient pressure.

9. The method of claim 8, wherein the greater than ambient pressure is provided by heating the solution in a sealed environment.

10. The method of any one of claims 1 to 9, wherein the heating is at a temperature of about 140 °C to about 200 °C.

11. The method of claim 10, wherein the heating is at a temperature of about 180 °C.

12. The method of any one of claims 1 to 11, wherein the heating is for a time of about 1 hour to about 24 hours.

13. The method of claim 12, wherein the heating is for a time of about 8 hours.

14. The method of any one of claims 1 to 13, wherein the cobalt (II) compound and the chromium (III) compound are salts soluble in the alcohol.

15. The method of claim 14, wherein the cobalt (II) compound and the chromium (III) compound are nitrate salts.

16. The method of claim 15, wherein the cobalt (II) compound is cobalt (II) nitrate hexahydrate and the chromium (III) compound is chromium (III) nitrate nonahydrate.

17. The method of any one of claims 1 to 16, wherein the method further comprises washing the separated precipitate prior to the calcining.

18. The method of any one of claims 1 to 17, wherein the method further comprises drying the separated and optionally washed precipitate prior to the calcining.

19. The method of any one of claims 1 to 18, wherein the calcining is at a temperature of about 400 °C to about 600 °C.

20. The method of claim 19, wherein the calcining is at a temperature of about 500 °C.

21. The method of any one of claims 1 to 20, wherein the calcining is for a time of about 1 hour to about 15 hours.

22. The method of claim 21, wherein the calcining is for a time of about 3 hours.

23. $CoCr_2O_4$ nanoparticles prepared by the method of any one of claims 1 to 22.

24. $CoCr_2O_4$ nanoparticles having a Brunauer-Emmett-Teller (BET) specific surface area at 77 K of at least 50 m^2/g.

25. The nanoparticles of claim 23 or 24, wherein the nanoparticles have a BET specific surface area of at least 90, 95 or 100 m^2/g.

26. The nanoparticles of any one of claims 23 to 25, wherein the nanoparticles are generally spherical.

27. The nanoparticles of any one of claims 23 to 26, wherein the nanoparticles have a diameter of about 300 nm to about 900 nm.

28. The nanoparticles of any one of claims 23 to 27, wherein the nanoparticles are polycrystals having a crystallite size of about 6 nm to about 12 nm.

29. The nanoparticles of any one of claims 23 to 27, wherein the nanoparticles are polycrystals having a crystallite size of about 10 nm.

30. The nanoparticles of any one of claims 23 to 29, wherein the nanoparticles are generally smooth and substantially free of adhered Co_3O_4 nanostructures.

31. The nanoparticles of any one of claims 23 to 29, wherein the nanoparticles are generally smooth and substantially free of Co_3O_4 and Cr_2O_3.

32. Use of the nanoparticles of any one of claims 23 to 31 as a catalyst for combustion of methane.

33. A method for catalytic combustion of methane comprising contacting a gaseous stream containing methane and oxygen with a catalyst comprising the nanoparticles of any one of claims 23 to 31.

34. The method of claim 33, wherein the temperature during the contacting is in a range of from about 20 °C to about 600 °C.

35. The method of claim 34, wherein the temperature is less than about 500 °C.

36. The method of any one of claims 33 to 35, wherein the gaseous stream further comprises one or more of water vapor and SO_x

37. The method of any one of claims 33 to 36, wherein the catalyst is present in a catalytic converter.

38. The method of claim 37, wherein the catalytic converter is in a vehicle and the gaseous stream is the exhaust of the vehicle.

39. The method of claim 38, wherein the vehicle is fueled by natural gas.

40. The method of claim 37, wherein the catalytic converter is in a stationary power generator and the gaseous stream is the exhaust of the stationary power generator.

41. The method of claim 40, wherein the stationary power generator is fueled by natural gas.

42. A supported catalyst comprising a solid catalyst support; and a coating comprising the nanoparticles of any one of claims 23 to 31.

43. The supported catalyst of claim 42, wherein the support comprises a bed of alumina, silica, silicon carbide, metal oxide, ceramic, or steatite particles or pellets.

44. The supported catalyst of claim 42, wherein the support is a monolithic ceramic support.

45. The supported catalyst of claim 44, wherein the monolithic ceramic support comprises cordierite.

46. The supported catalyst of claim 42, wherein the support is a corrugated metal foil.

47. The supported catalyst of claim 44, 45 or 46, wherein the support forms a honeycomb structure.

48. The supported catalyst of any one of claims 42 to 47, wherein the coating further comprises a secondary support.

49. The supported catalyst of claim 48, wherein the secondary support comprises alumina.

50. A catalytic converter comprising a supported catalyst of any one of claims 42 to 49.

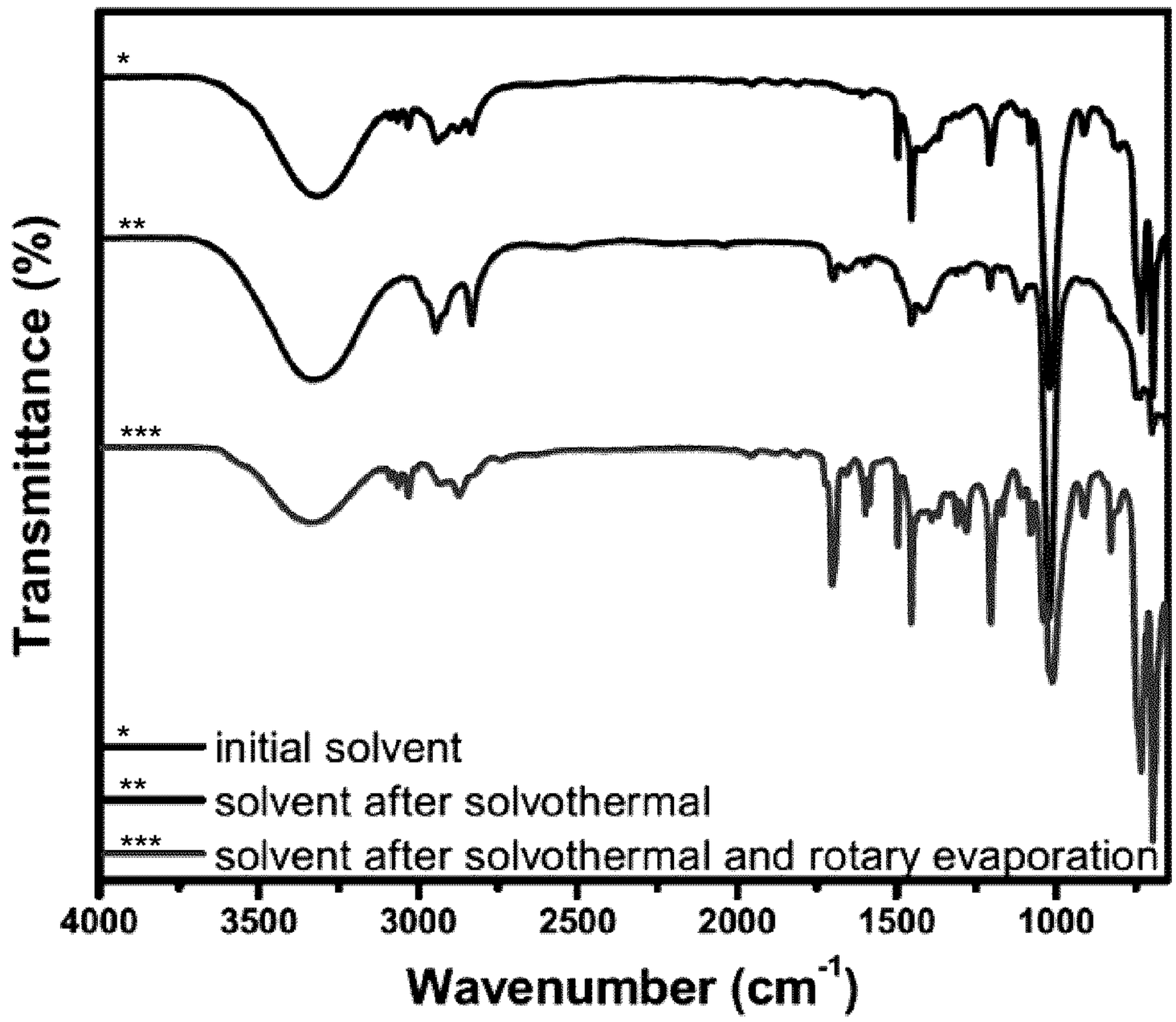

Transmittance (%)
*
**
***
initial solvent
solvent after solvothermal
solvent after solvothermal and rotary evaporation
4000
3500
3000
2500
2000
1500
1000
Wavenumber (cm-1)

FIG. 1

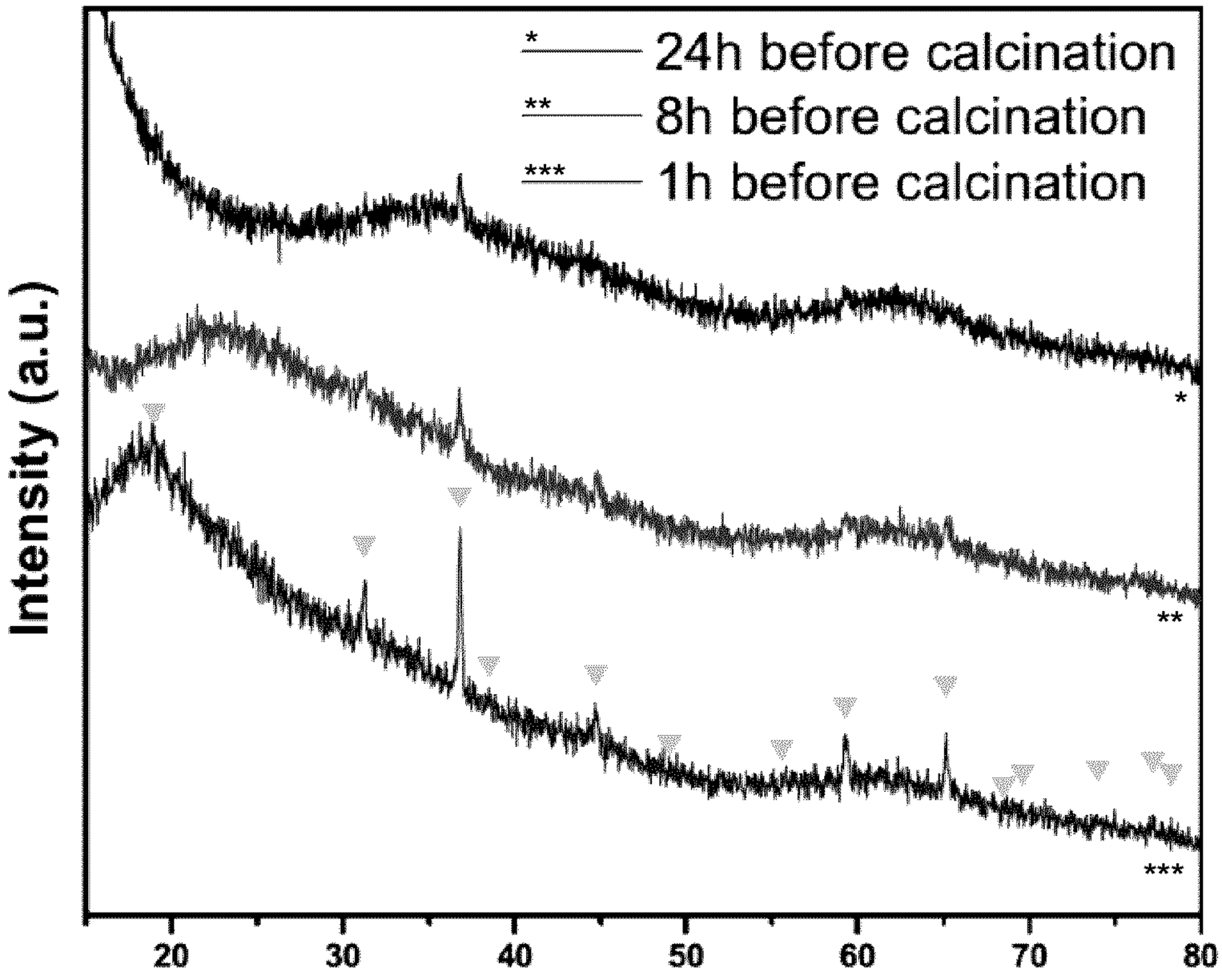

* 24h before calcination
** 8h before calcination
*** 1h before calcination
Intensity (a.u.)
*
**
***
20
30
40
50
60
70
80
2-Theta (°)

FIG. 2

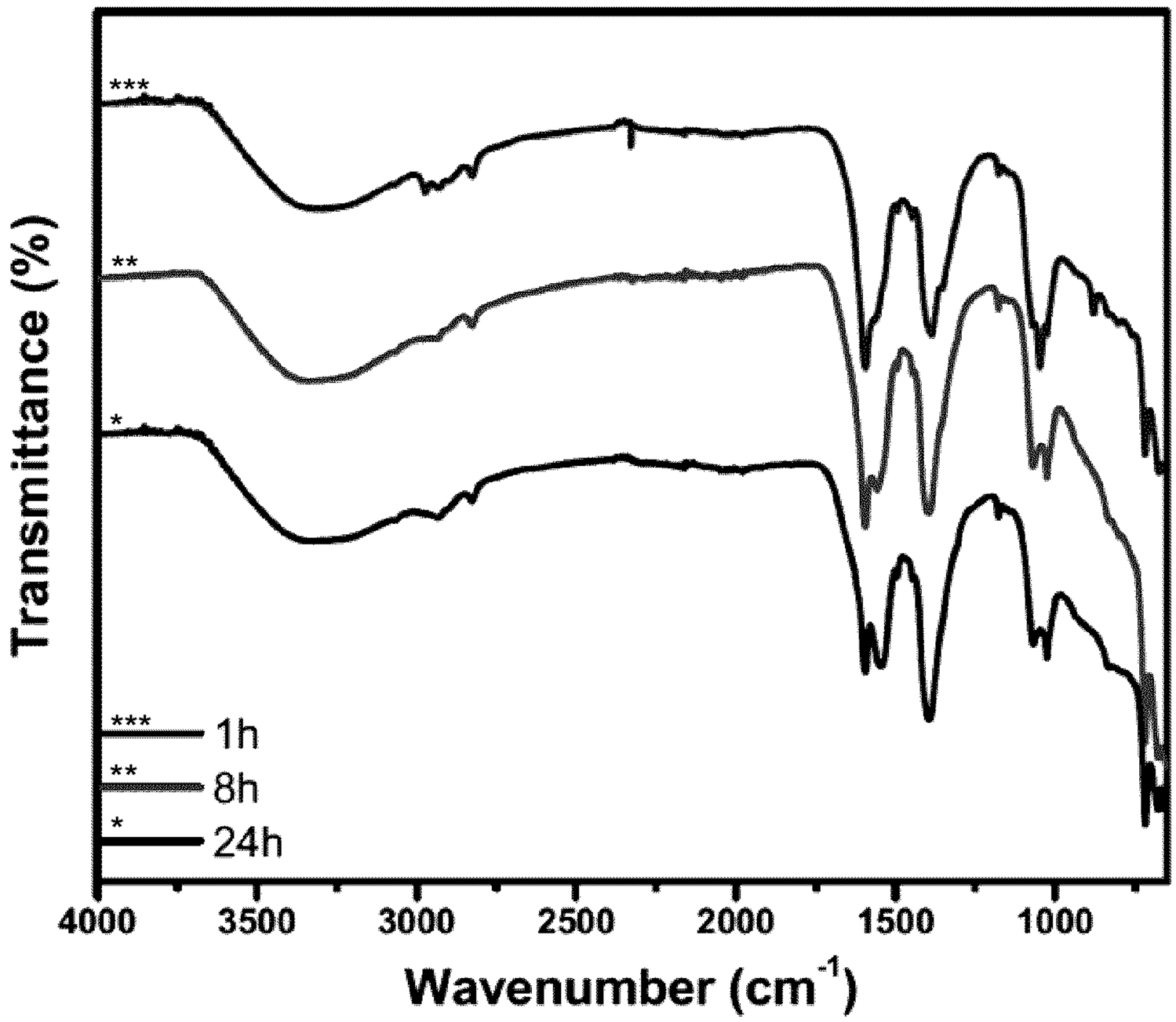

***
**
*
Transmittance (%)
***
1h
**
8h
*
24h
4000
3500
3000
2500
2000
1500
1000
Wavenumber (cm-1)

FIG. 3

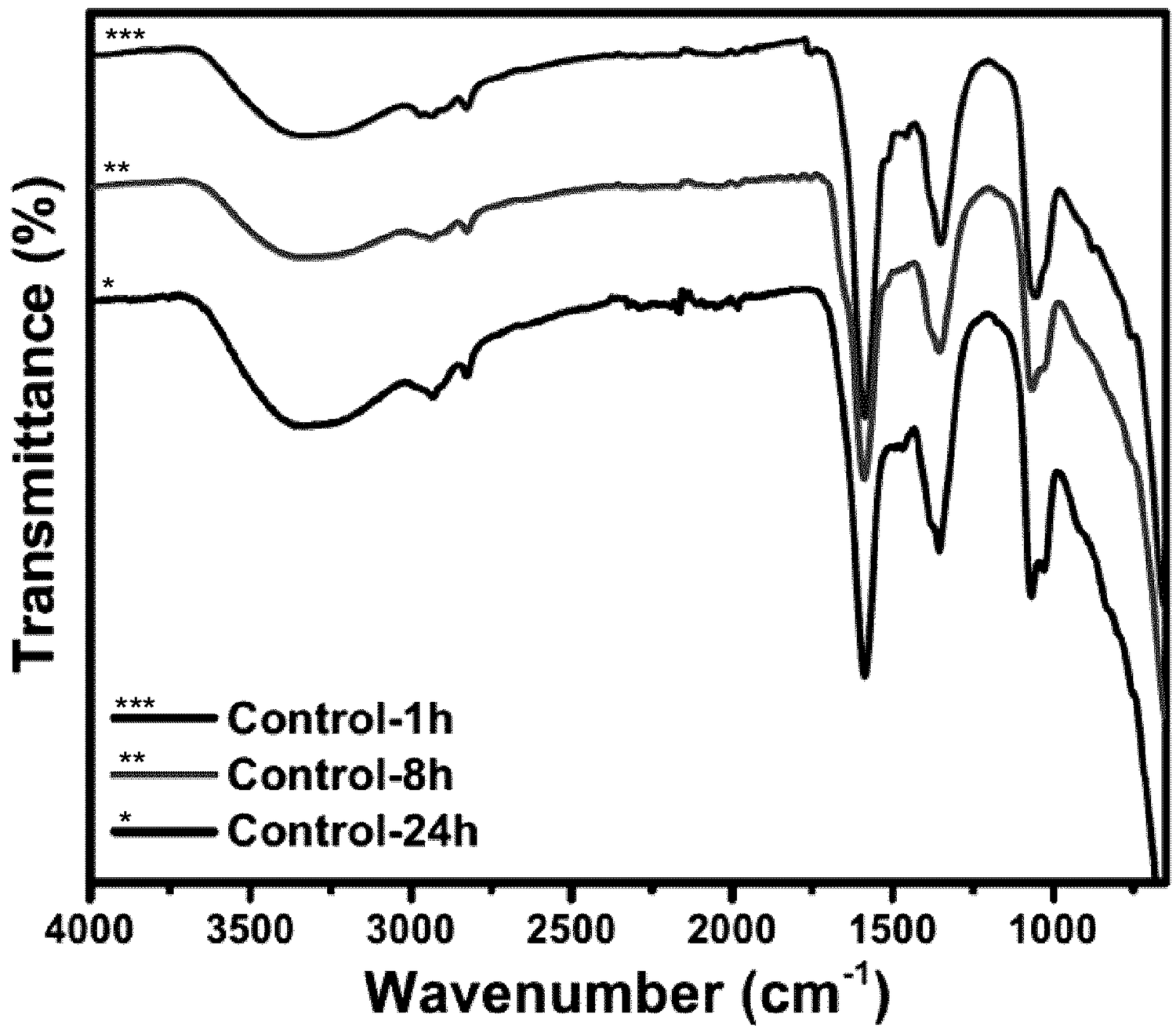

***
**
*
Transmittance (%)
*** Control-1h
** Control-8h
* Control-24h
4000
3500
3000
2500
2000
1500
1000
Wavenumber (cm-1)

FIG. 4

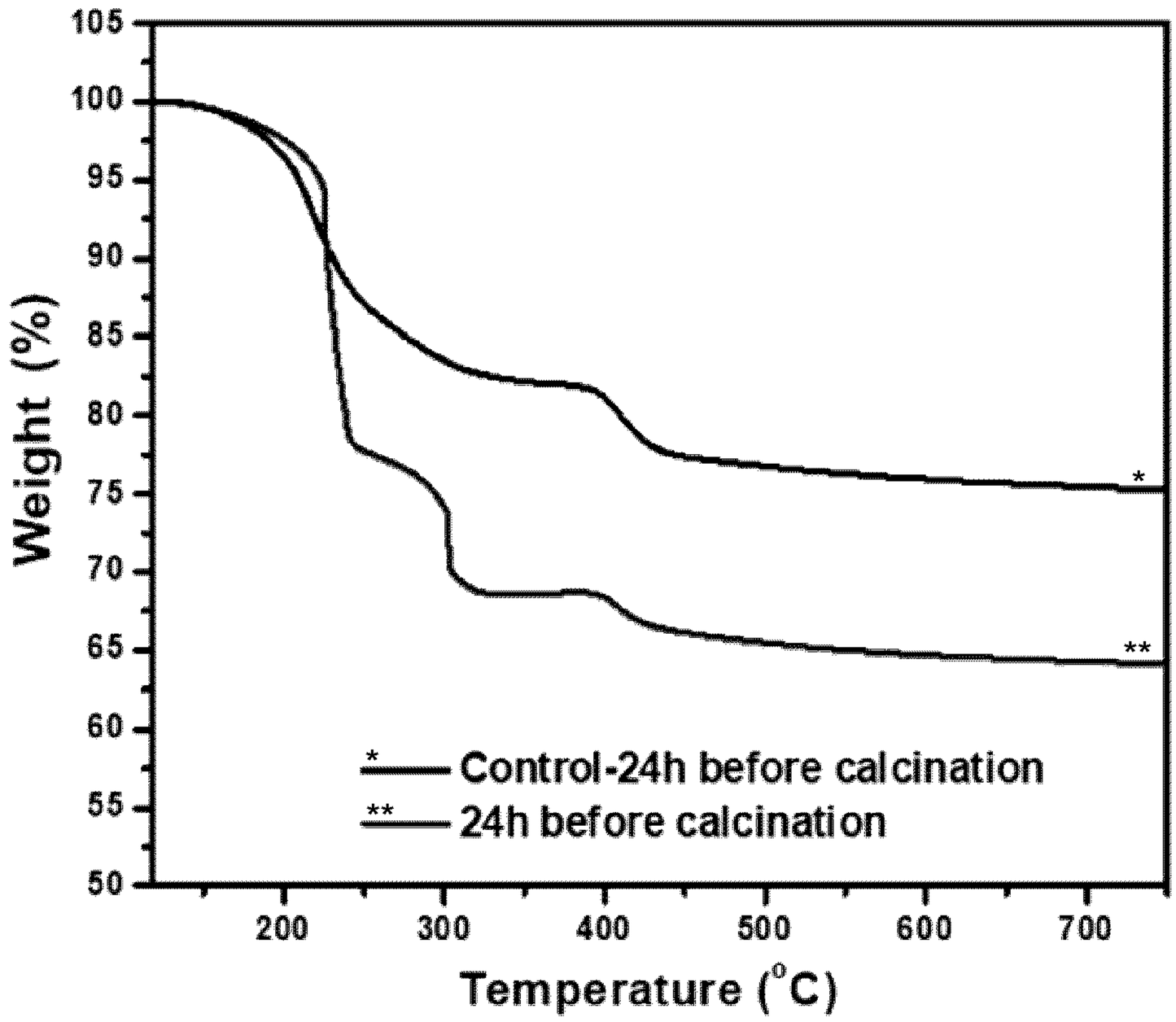

105
100
95
90
85
80
75
70
65
60
55
50
Weight (%)
200
300
400
500
600
700
Temperature (°C)
*
**
* Control-24h before calcination
** 24h before calcination

FIG. 5

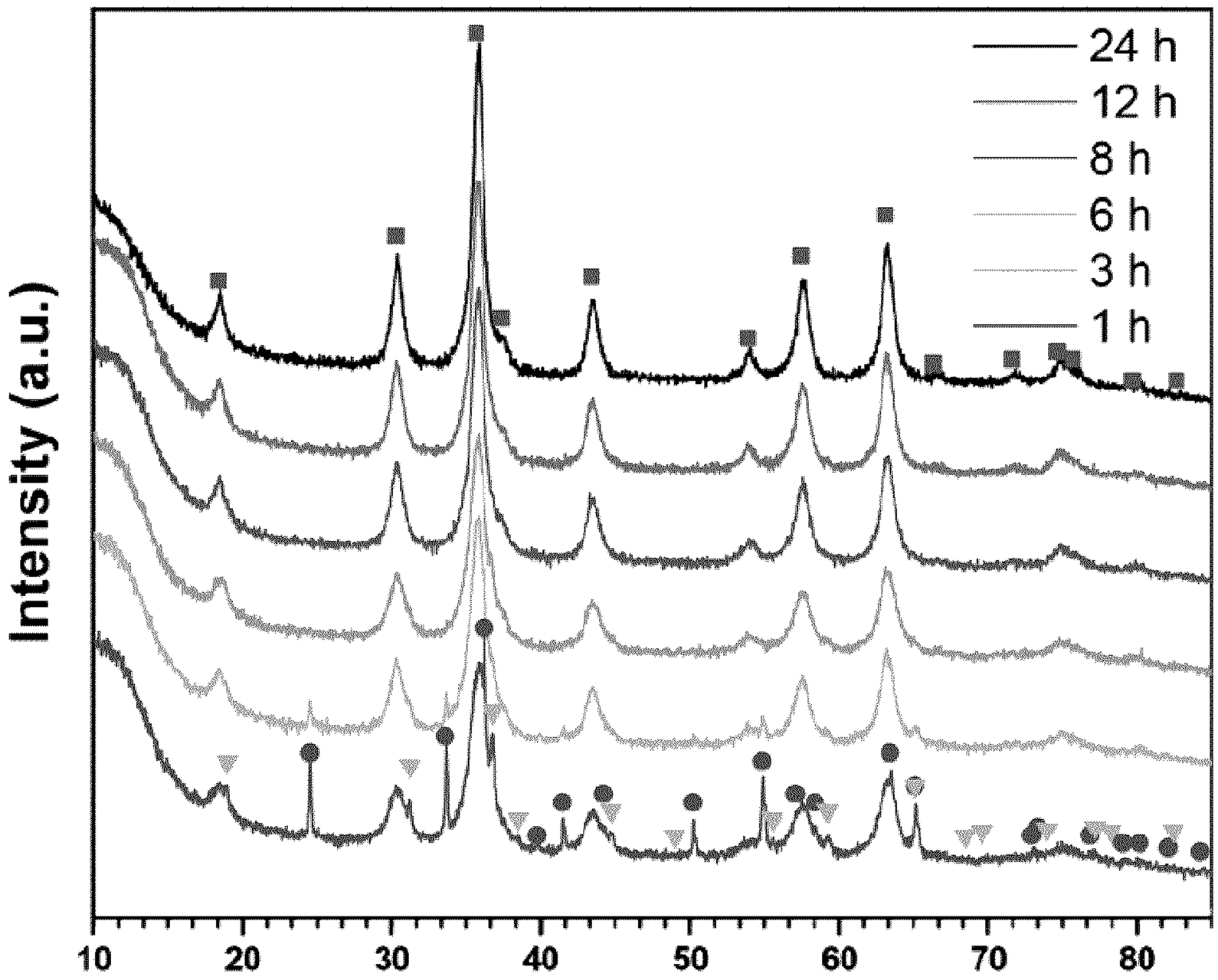


FIG. 6

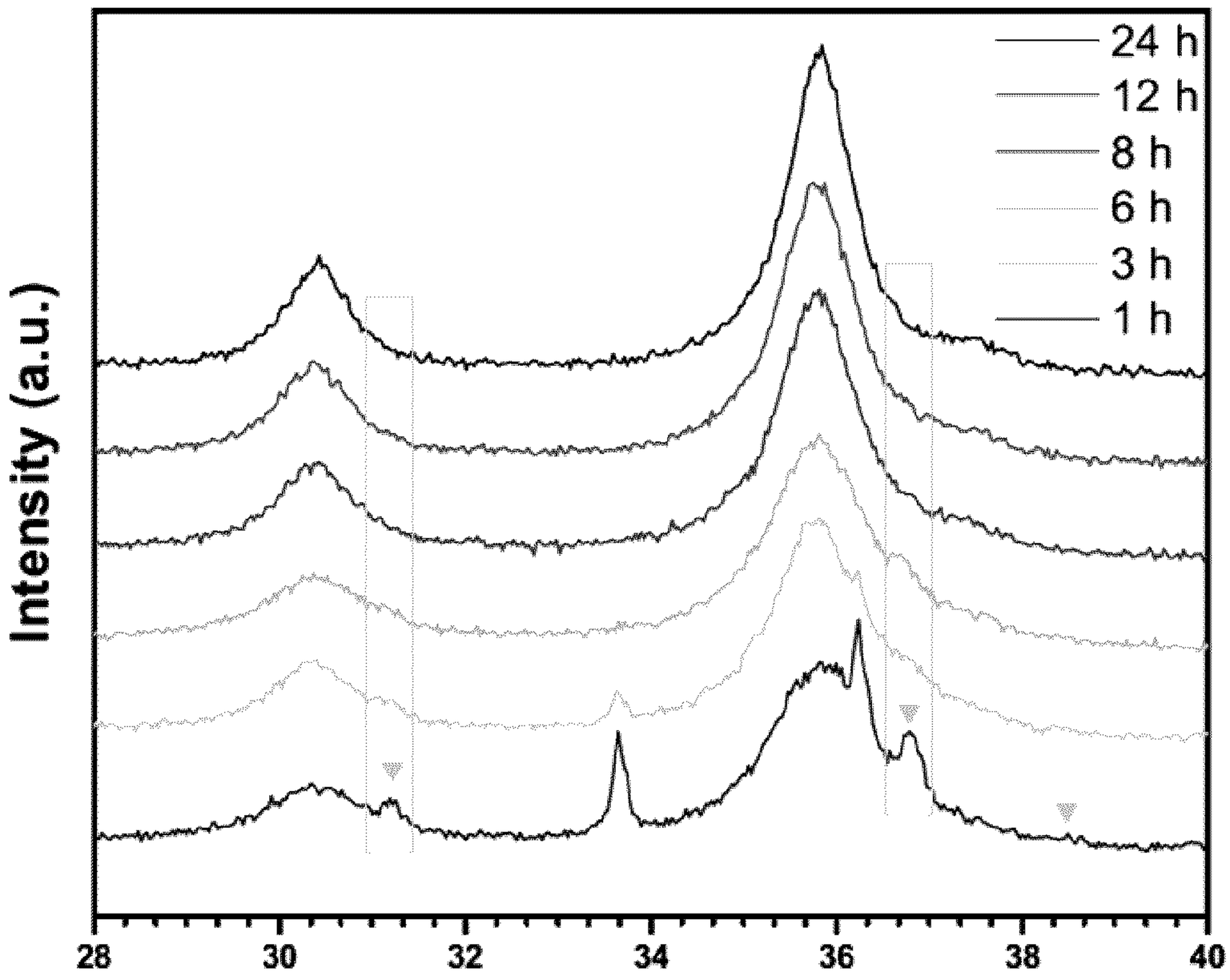


FIG. 7

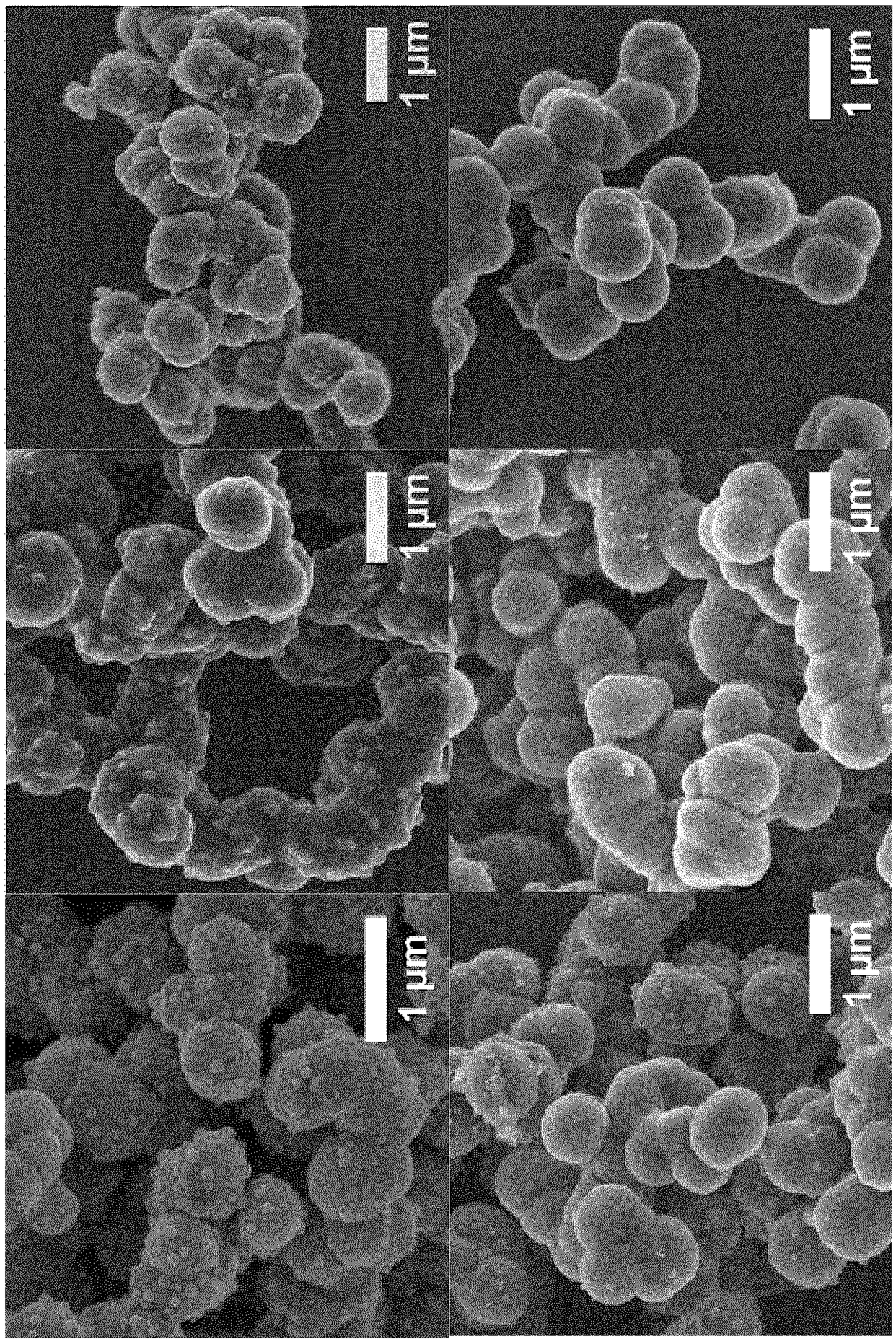


FIG. 8

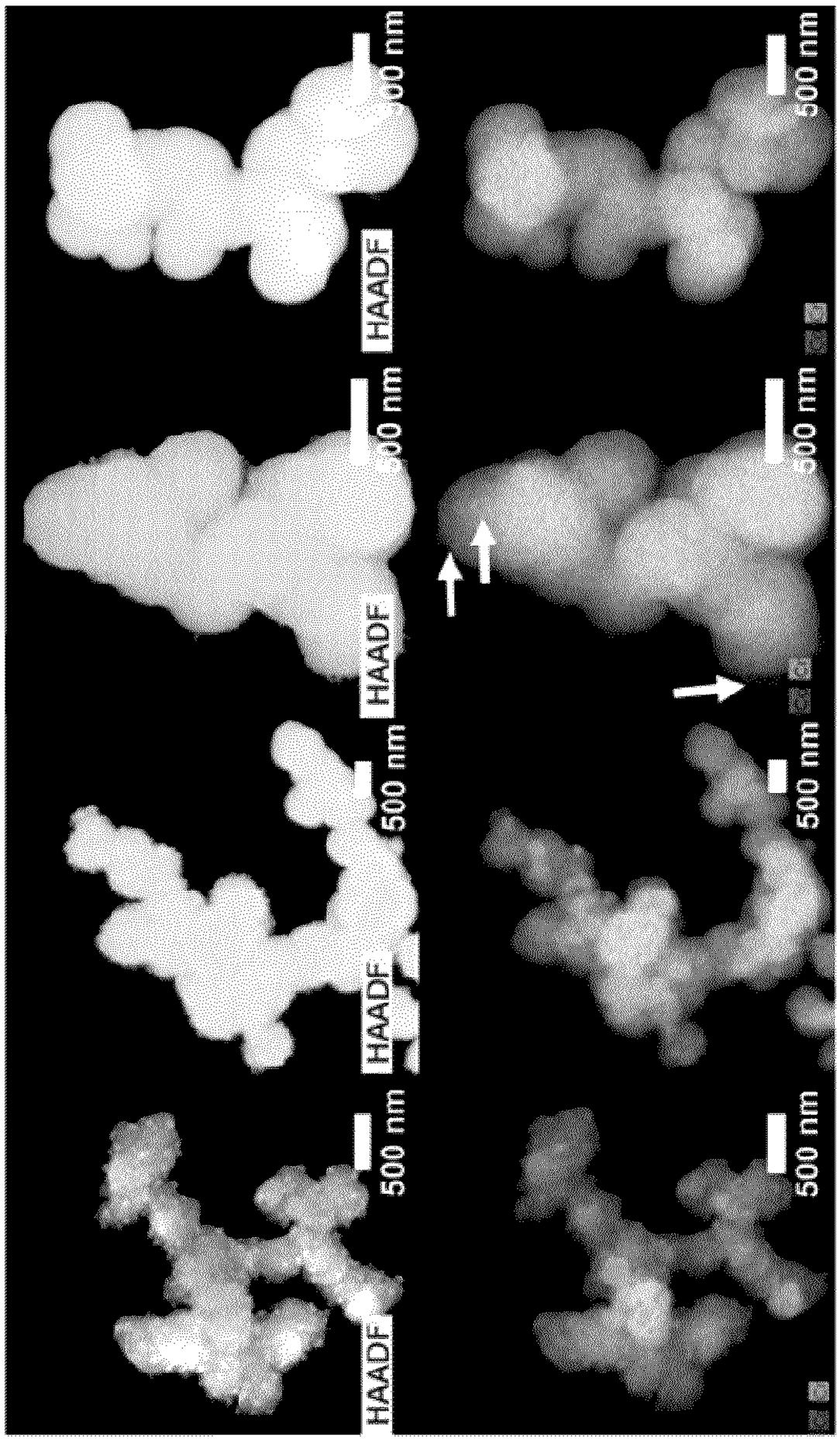

500 nm
HAADF
500 nm
HAADF
500 nm
HAADF
500 nm
HAADF
500 nm
HAADF
500 nm
HAADF

FIG. 9

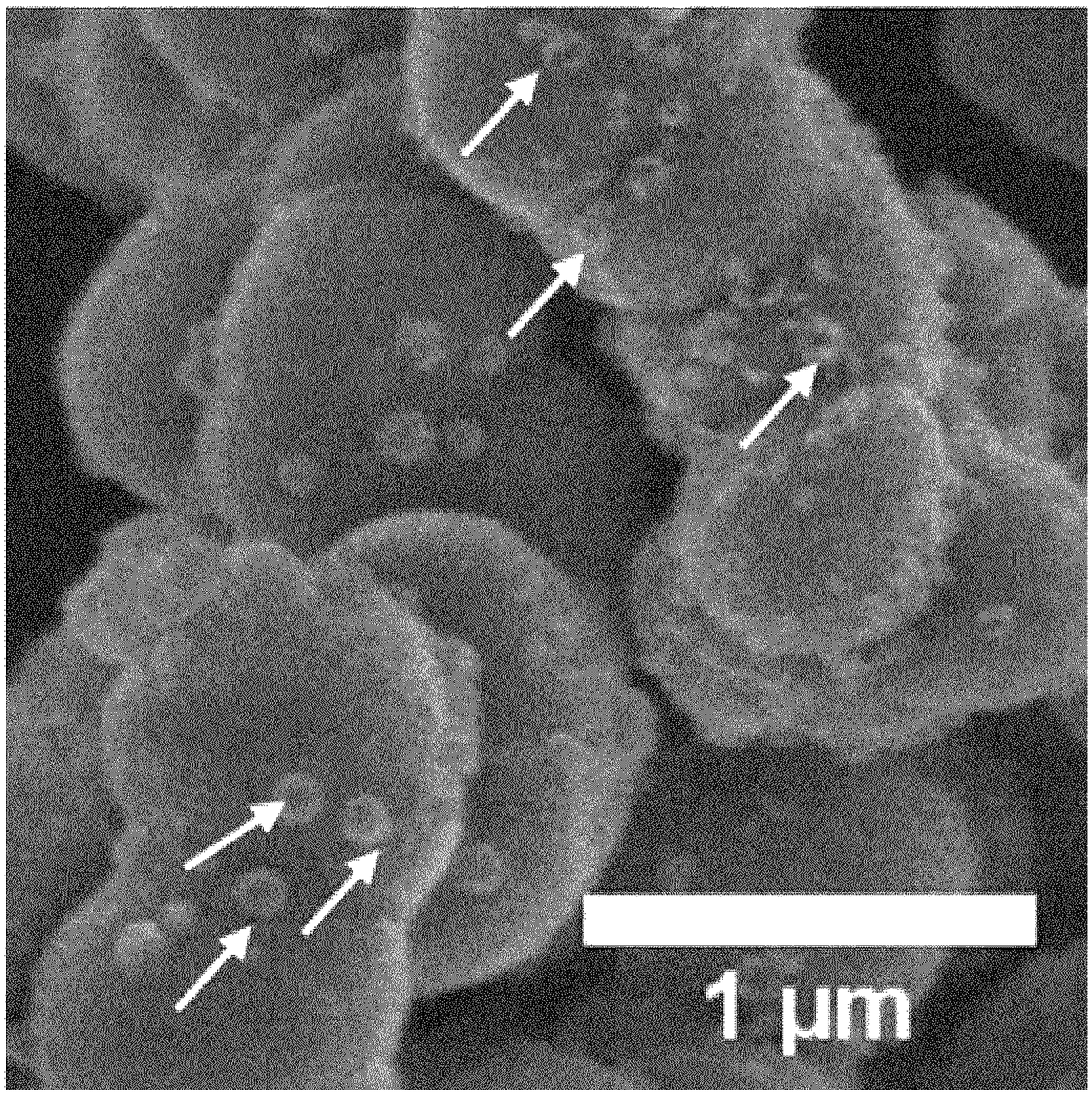


FIG. 10

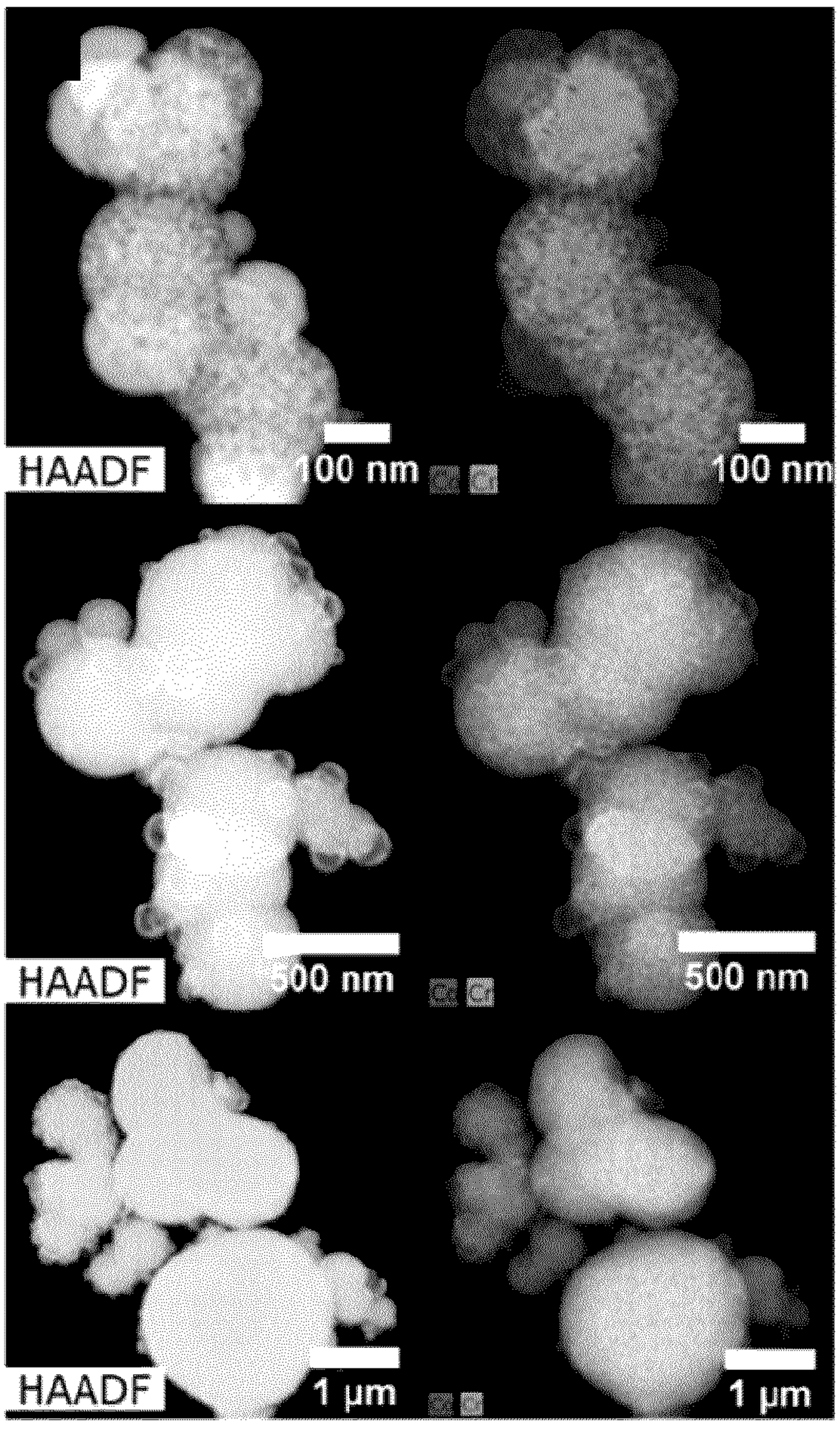


FIG. 11

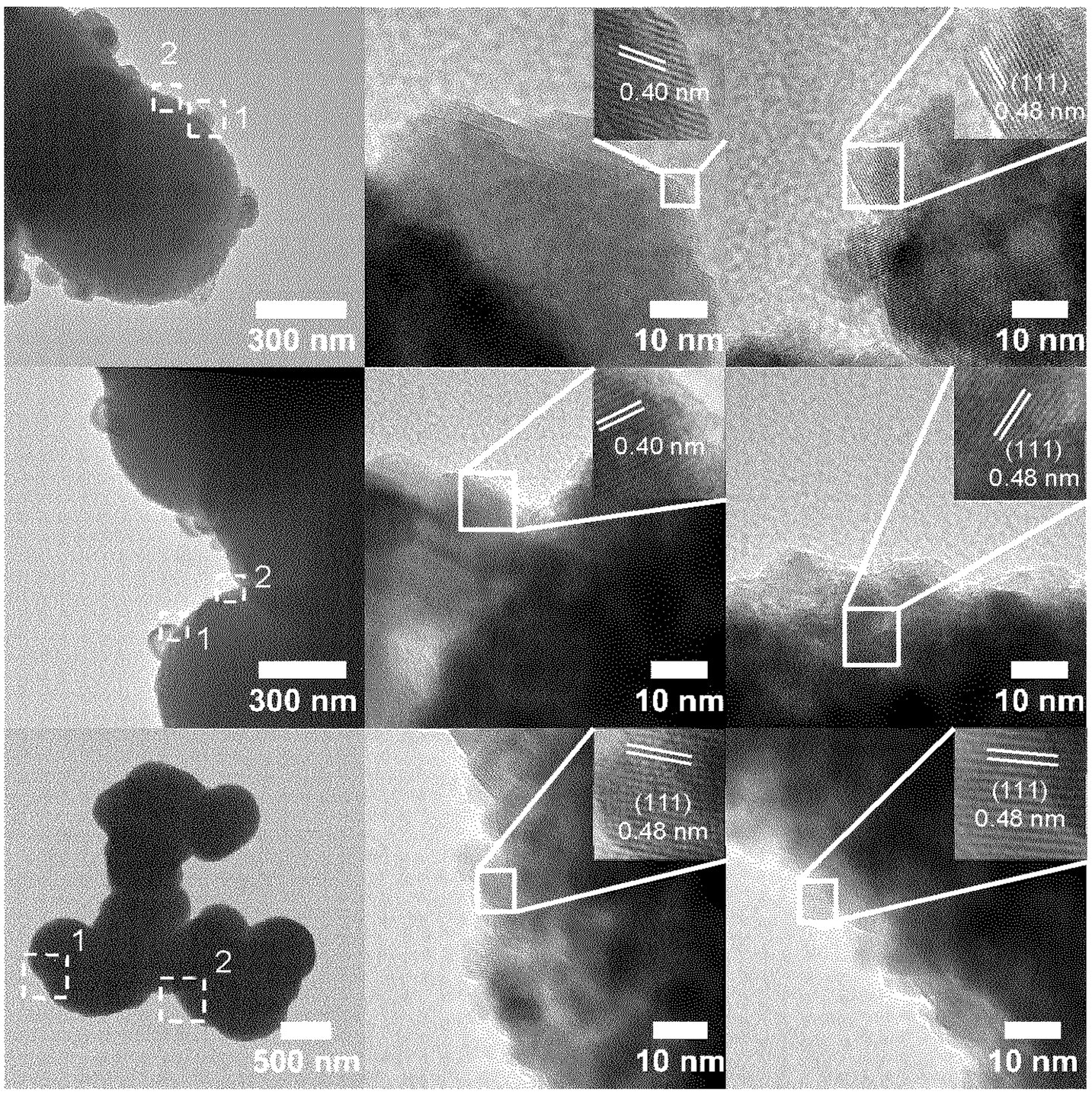

2
1
300 nm
10 nm
0.40 nm
(111)
0.48 nm
10 nm
2
1
300 nm
10 nm
0.40 nm
(111)
0.48 nm
10 nm
1
2
500 nm
10 nm
(111)
0.48 nm
10 nm

FIG. 12

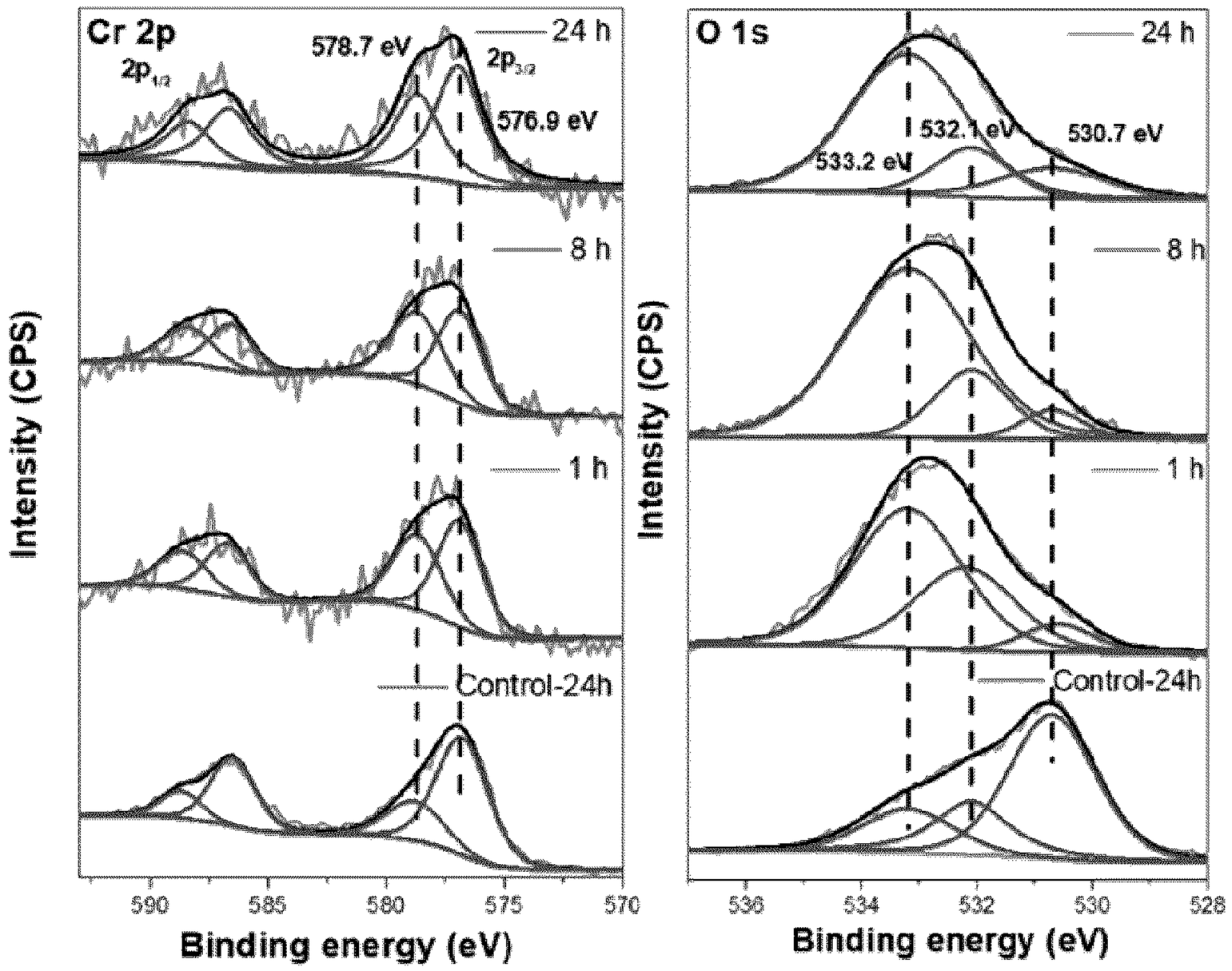

Cr 2p
578.7 eV
2p1/2
2p3/2
576.9 eV
24 h
8 h
1 h
Control-24h
Intensity (CPS)
590
585
580
575
570
Binding energy (eV)
O 1s
532.1 eV
533.2 eV
530.7 eV
24 h
8 h
1 h
Control-24h
Intensity (CPS)
536
534
532
530
528
Binding energy (eV)

FIG. 13

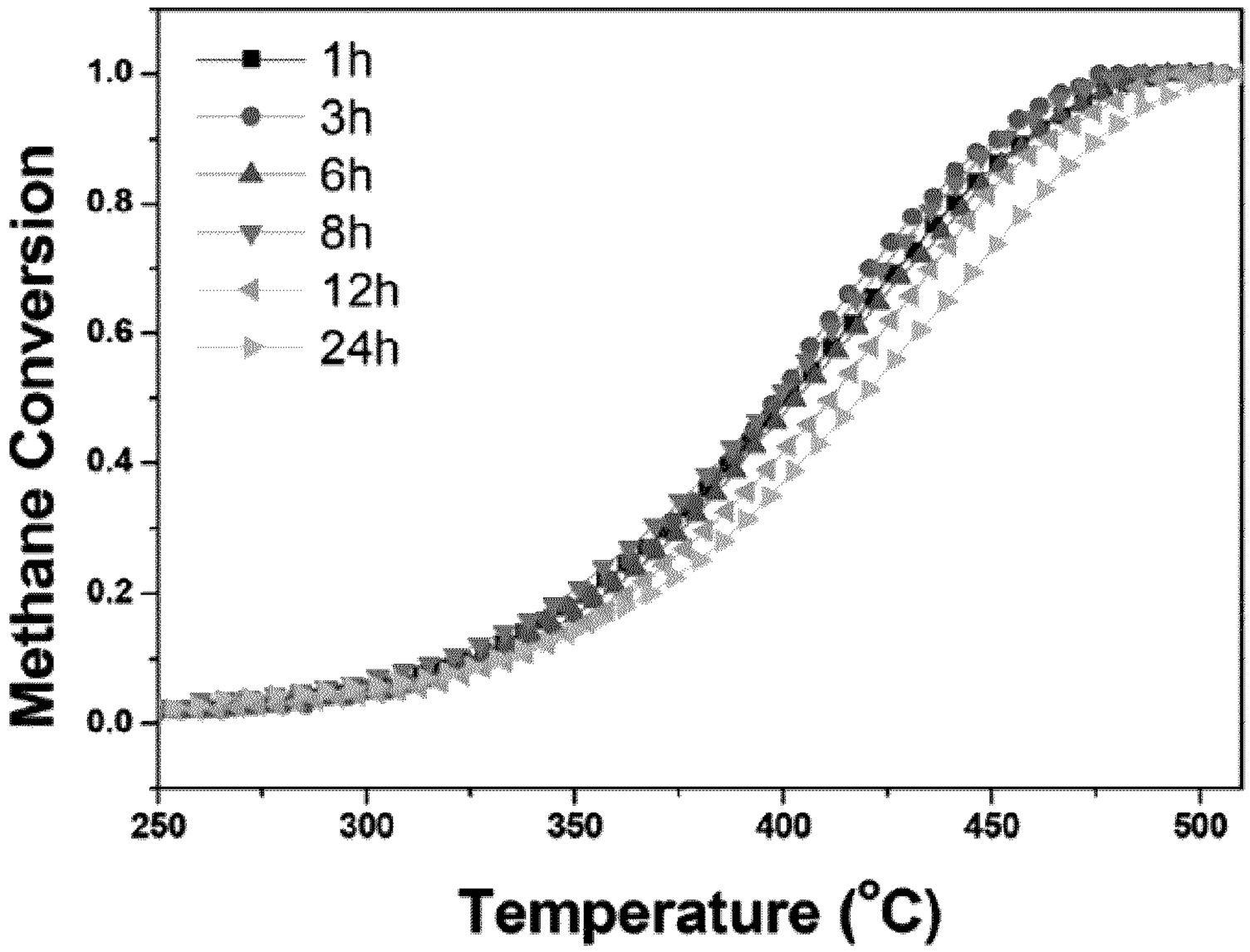

1h
3h
6h
8h
12h
24h
Methane Conversion
1.0
0.8
0.6
0.4
0.2
0.0
250
300
350
400
450
500
Temperature (°C)

FIG. 14

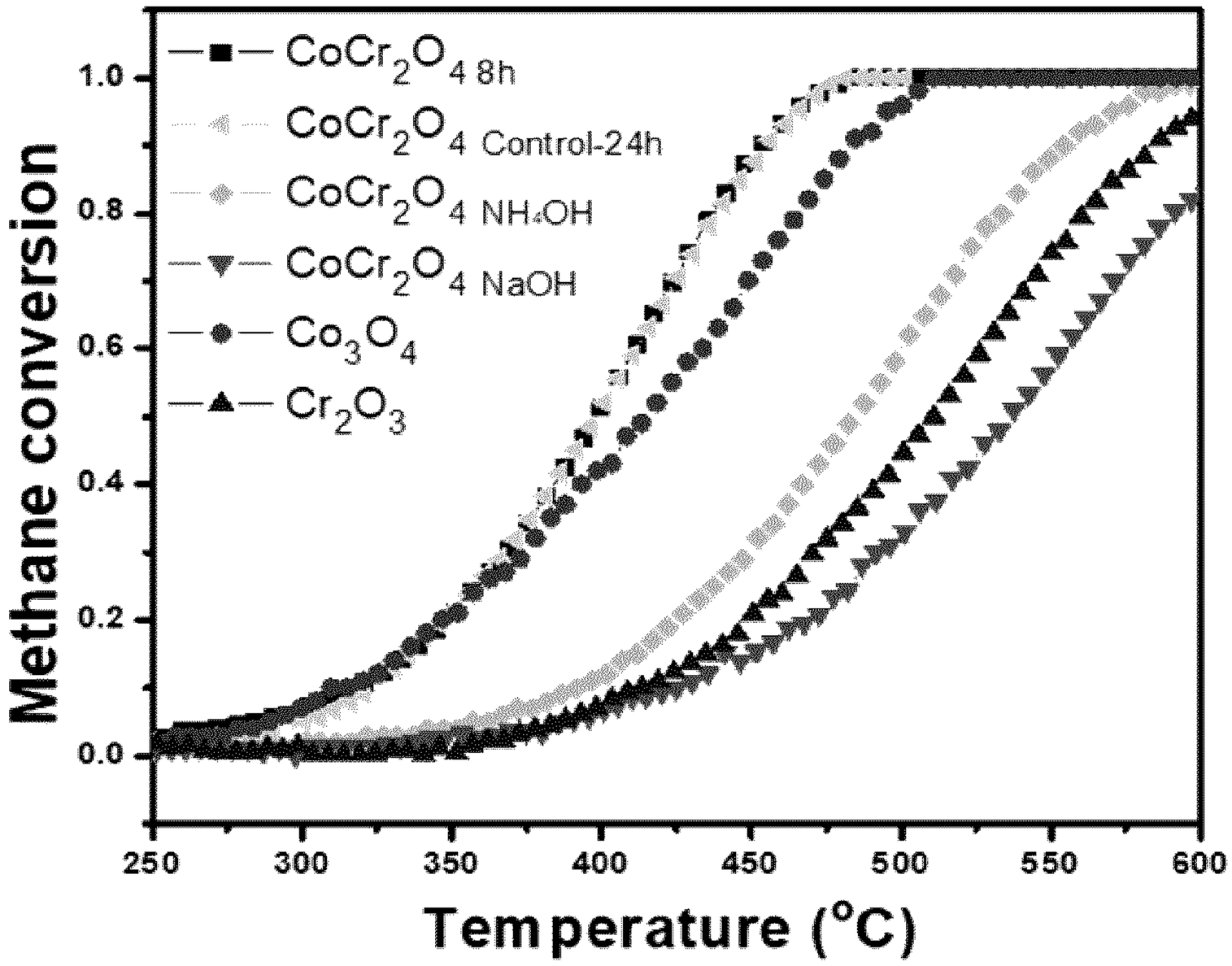

$CoCr_2O_4$ 8h
$CoCr_2O_4$ Control-24h
$CoCr_2O_4$ NH_4OH
$CoCr_2O_4$ NaOH
Co_3O_4
Cr_2O_3
Methane conversion
1.0
0.8
0.6
0.4
0.2
0.0
250
300
350
400
450
500
550
600
Temperature (°C)

FIG. 15

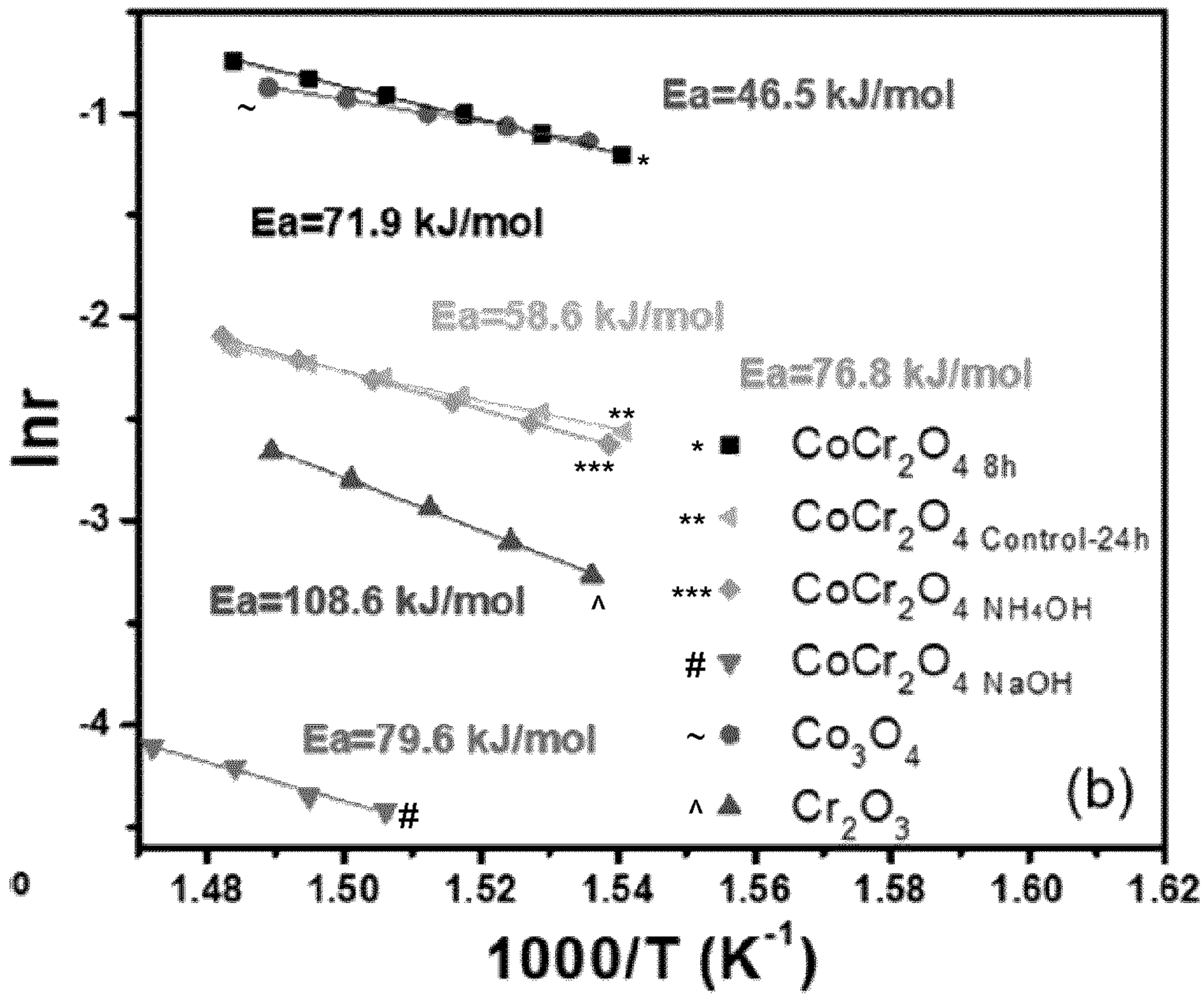

Ea=46.5 kJ/mol
Ea=71.9 kJ/mol
Ea=58.6 kJ/mol
Ea=76.8 kJ/mol
Ea=108.6 kJ/mol
Ea=79.6 kJ/mol
lnr
-1
-2
-3
-4
0
1.48
1.50
1.52
1.54
1.56
1.58
1.60
1.62
1000/T (K-1)
* CoCr2O4 8h
** CoCr2O4 Control-24h
*** CoCr2O4 NH4OH
# CoCr2O4 NaOH
~ Co3O4
^ Cr2O3
(b)

FIG. 16

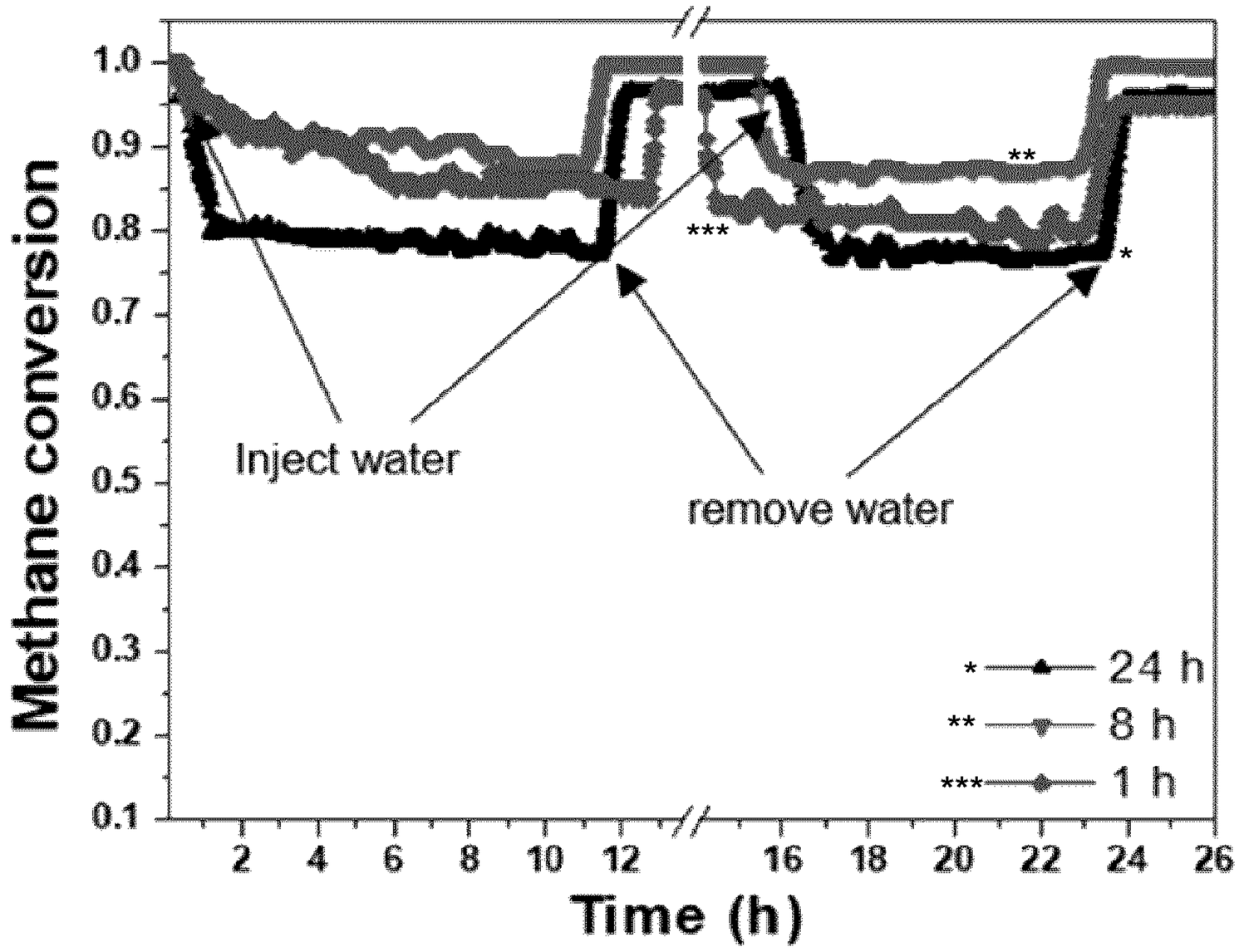

Methane conversion
1.0
0.9
0.8
0.7
0.6
0.5
0.4
0.3
0.2
0.1
2
4
6
8
10
12
16
18
20
22
24
26
Time (h)
Inject water
remove water
*
**
***
* 24 h
** 8 h
*** 1 h

FIG. 17

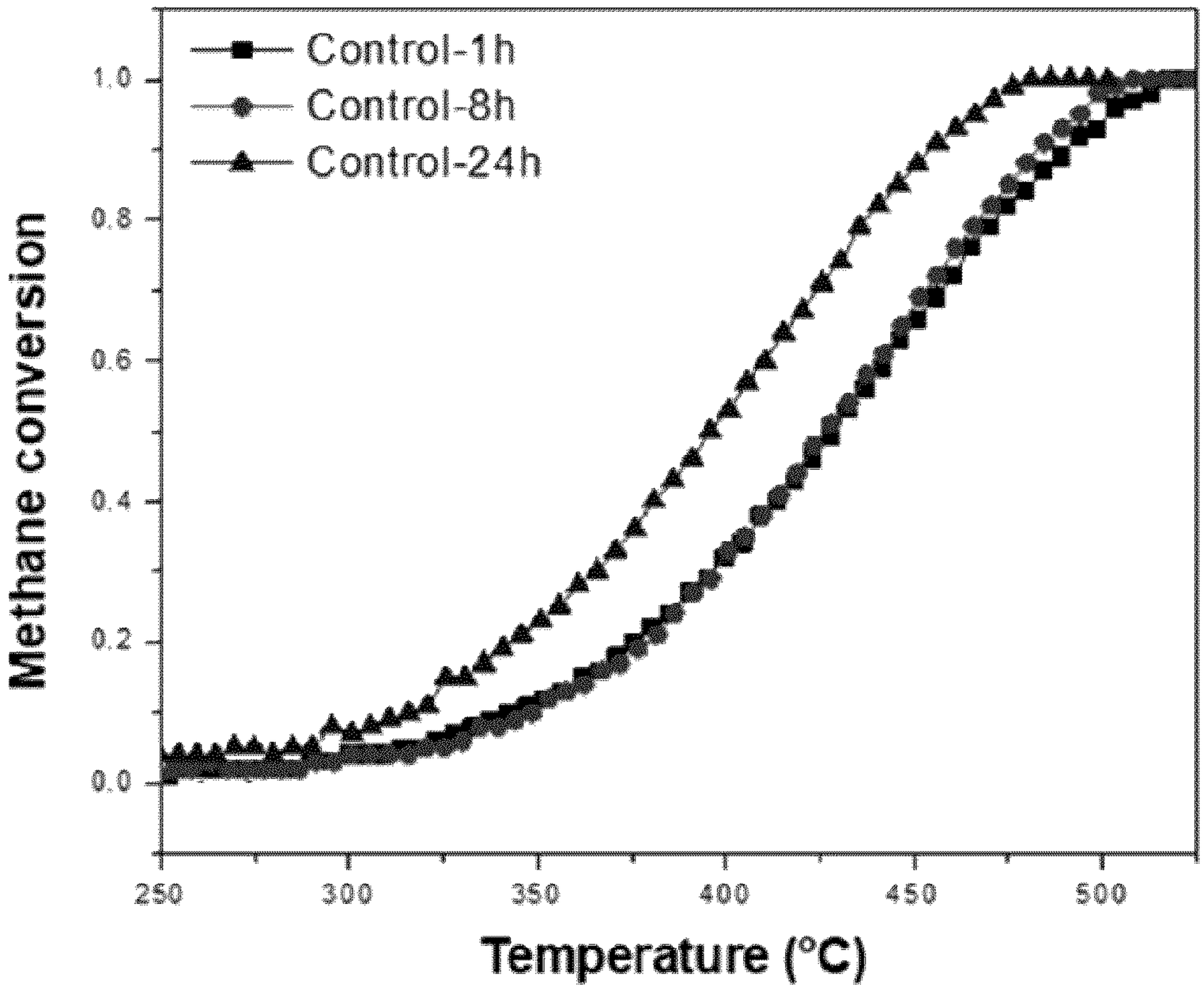

Control-1h
Control-8h
Control-24h
Methane conversion
0.0
0.2
0.4
0.6
0.8
1.0
250
300
350
400
450
500
Temperature (°C)

FIG. 18

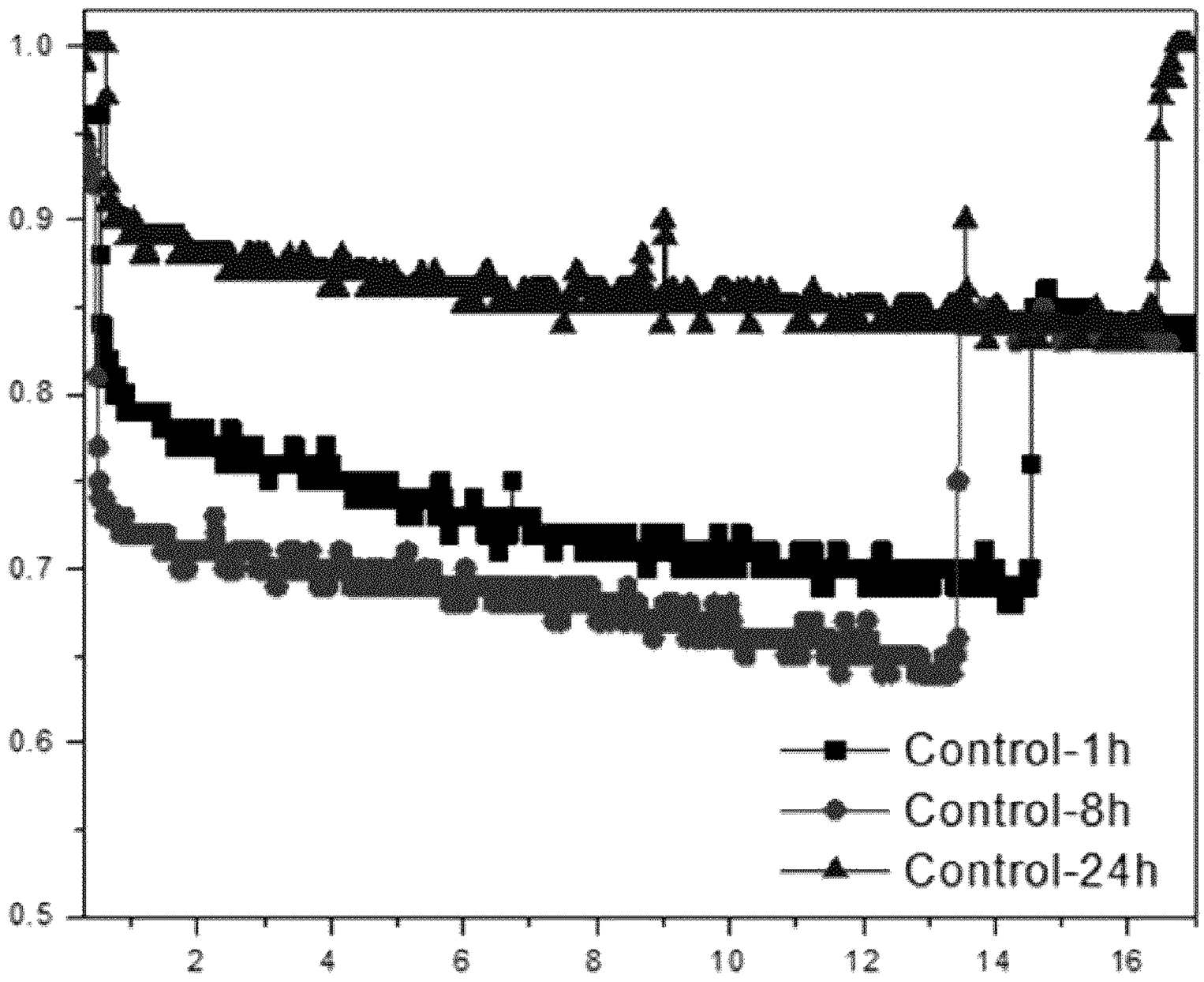

1.0
0.9
0.8
0.7
0.6
0.5
2
4
6
8
10
12
14
16
Time (h)
Control-1h
Control-8h
Control-24h

FIG. 19

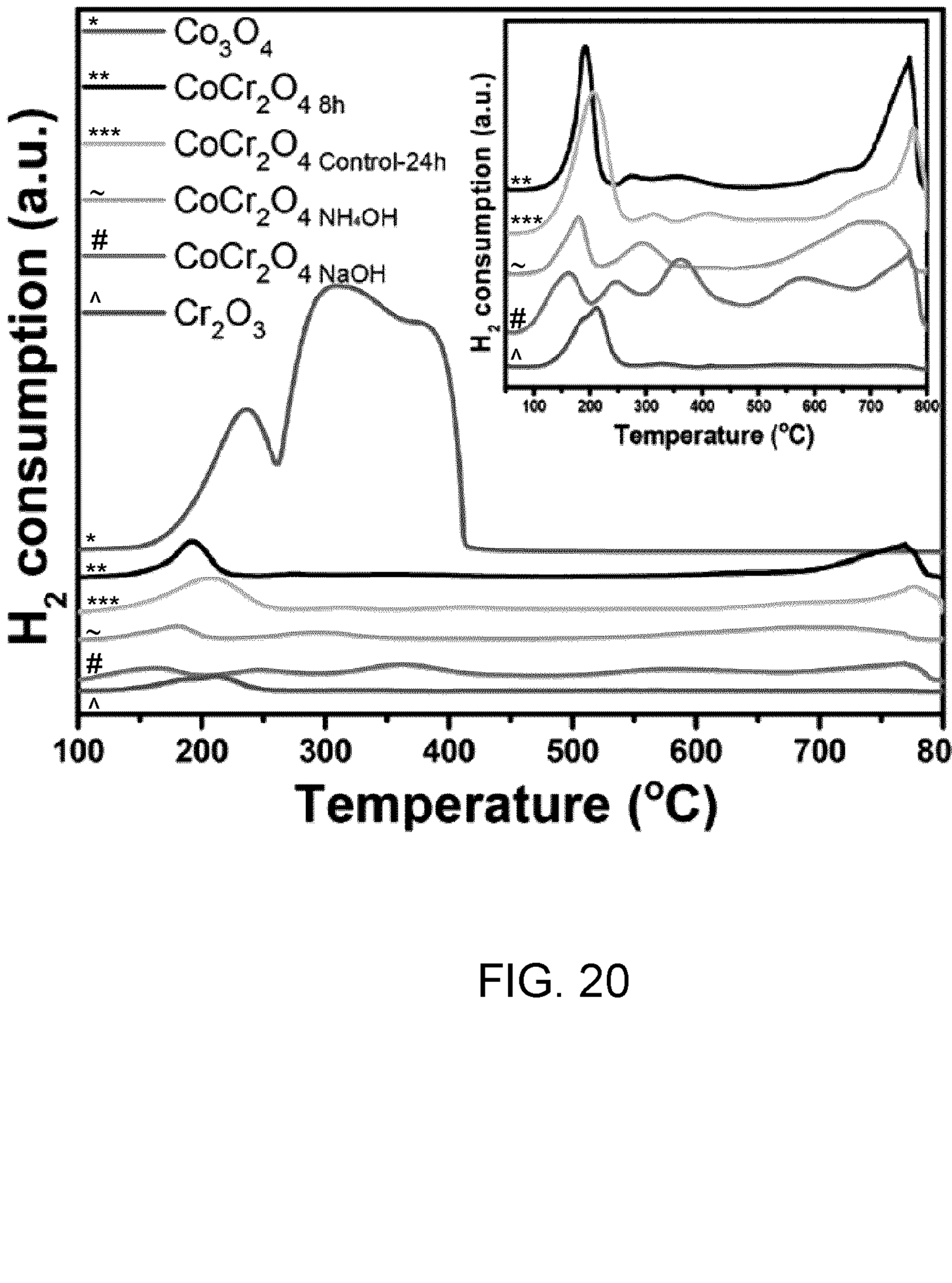

* Co_3O_4
** $CoCr_2O_4$ 8h
*** $CoCr_2O_4$ Control-24h
~ $CoCr_2O_4$ NH_4OH
# $CoCr_2O_4$ NaOH
^ Cr_2O_3
H_2 consumption (a.u.)
100 200 300 400 500 600 700 800
Temperature (°C)
H_2 consumption (a.u.)
Temperature (°C)

FIG. 20

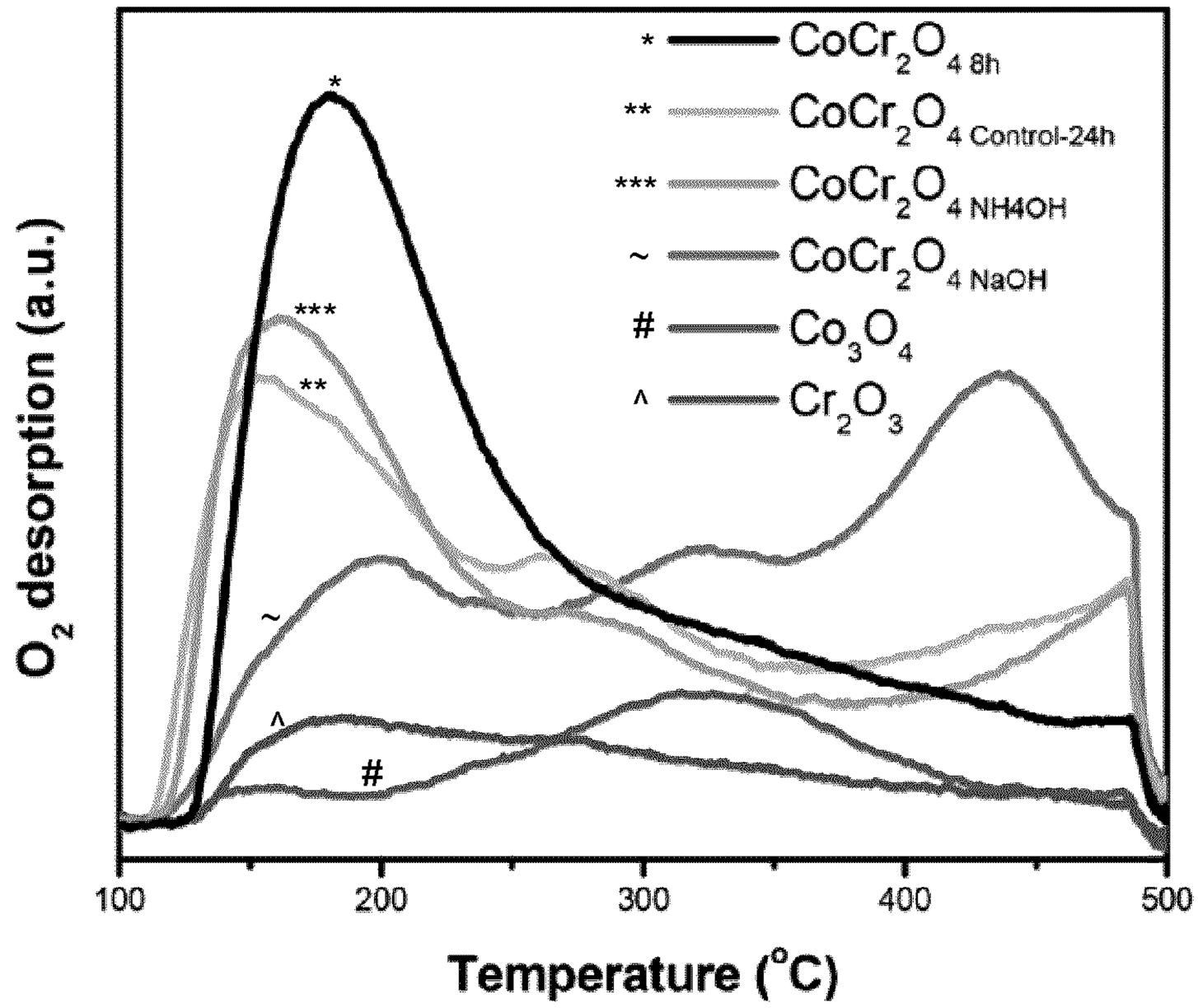

* CoCr2O4 8h
** CoCr2O4 Control-24h
*** CoCr2O4 NH4OH
~ CoCr2O4 NaOH
# Co3O4
^ Cr2O3
O2 desorption (a.u.)
100
200
300
400
500
Temperature (°C)

FIG. 21

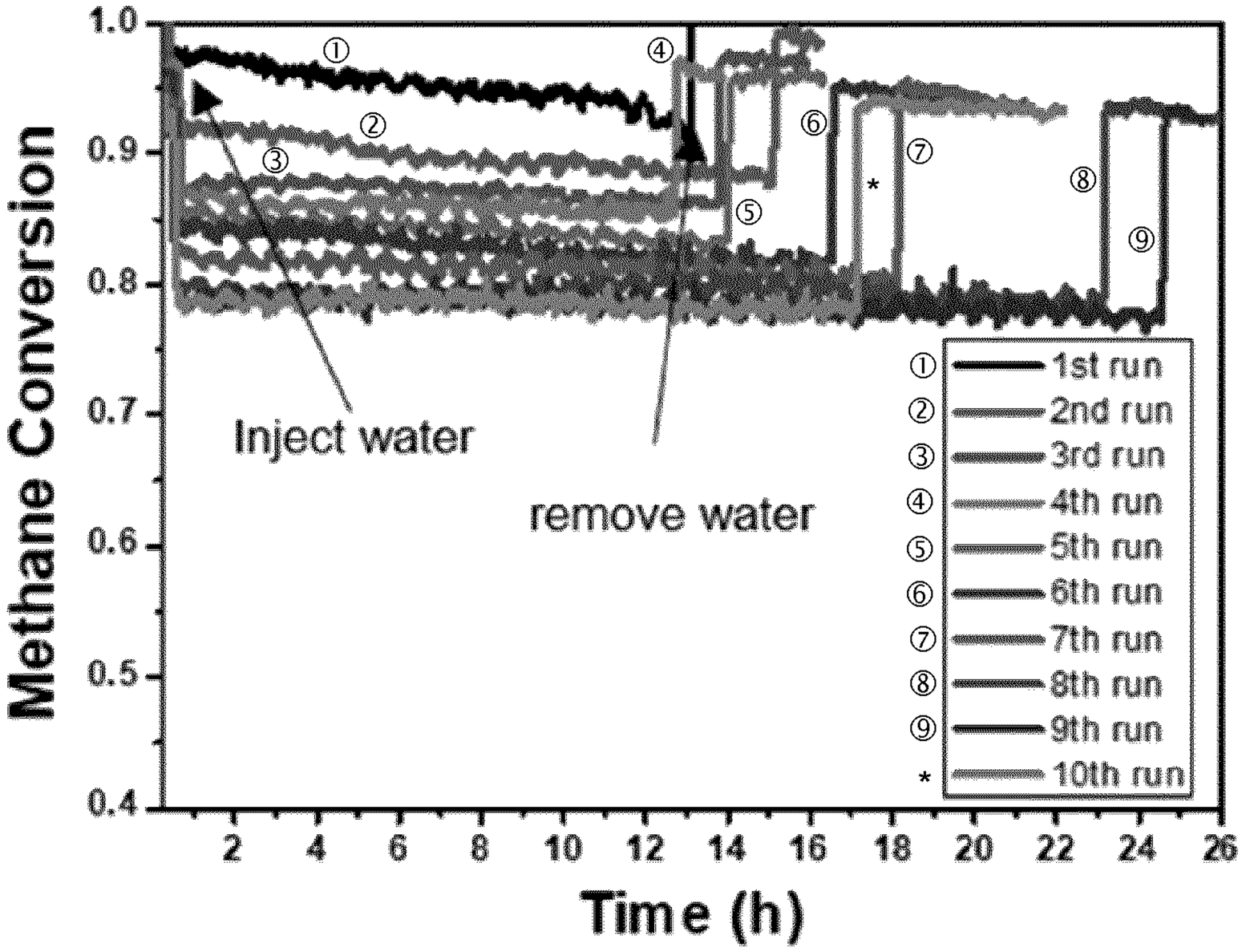

Methane Conversion
Time (h)
Inject water
remove water
① 1st run
② 2nd run
③ 3rd run
④ 4th run
⑤ 5th run
⑥ 6th run
⑦ 7th run
⑧ 8th run
⑨ 9th run
* 10th run

FIG. 22

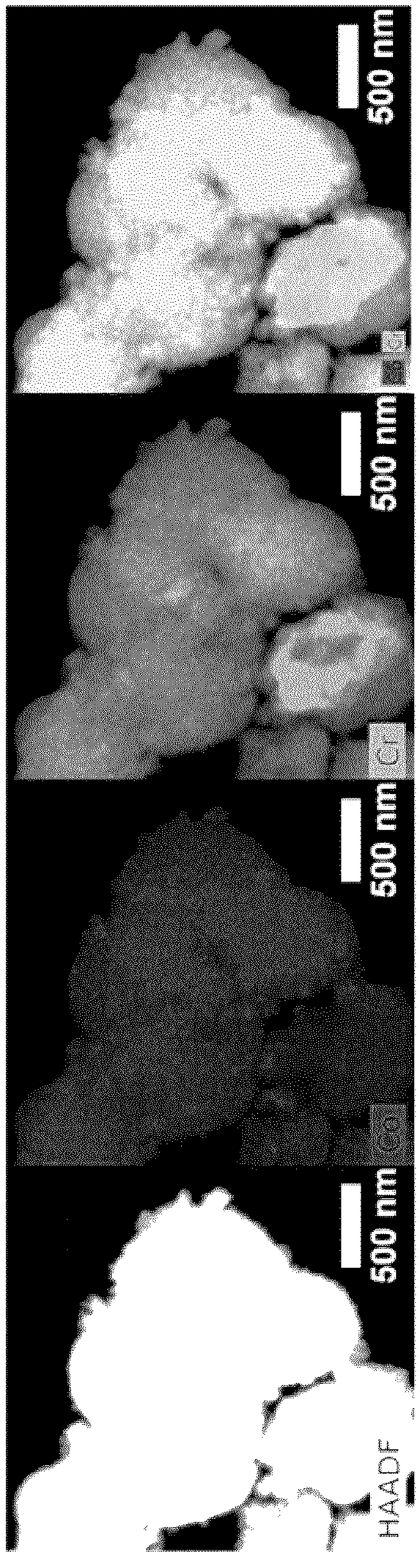


FIG. 23

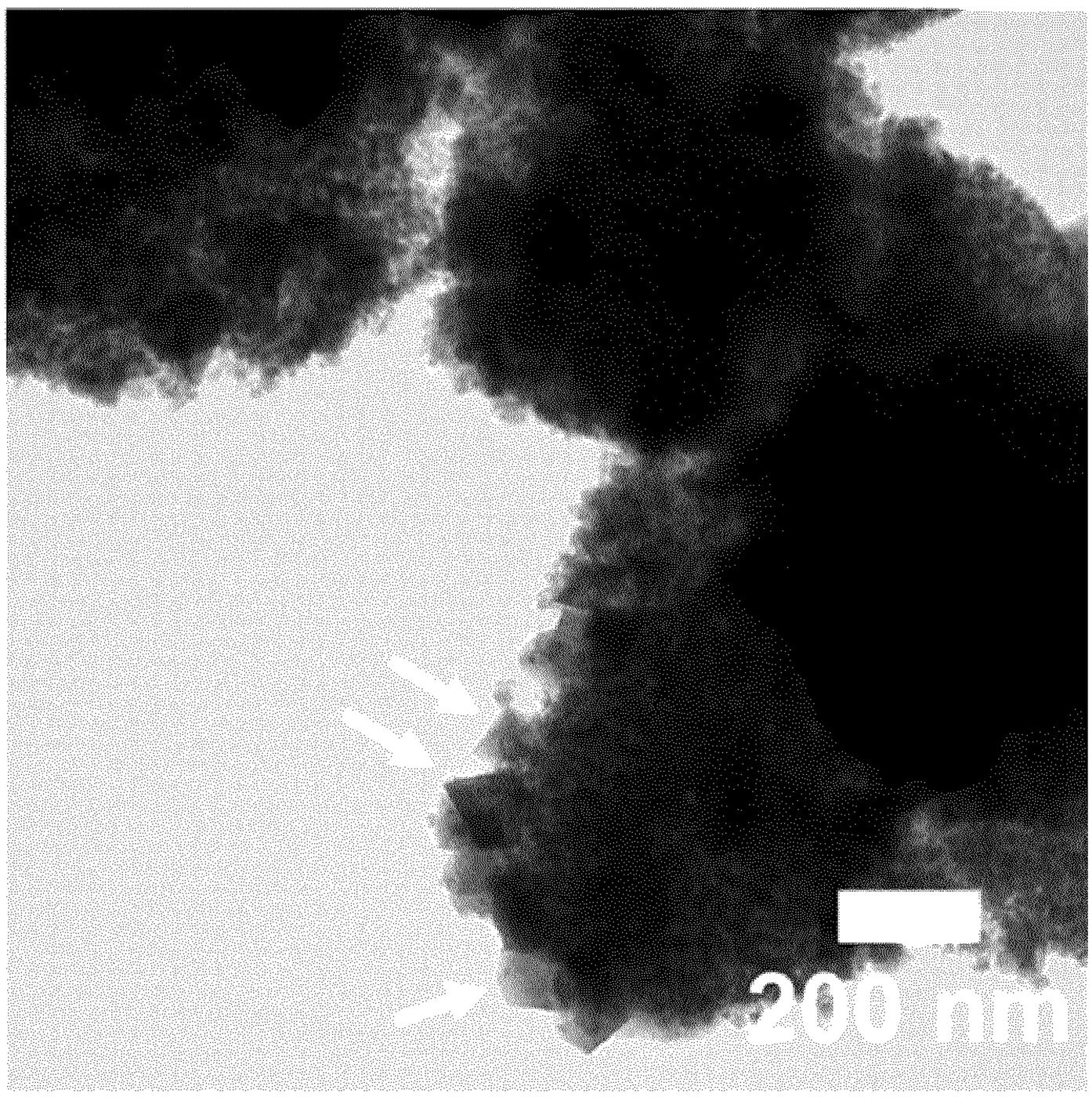


FIG. 24

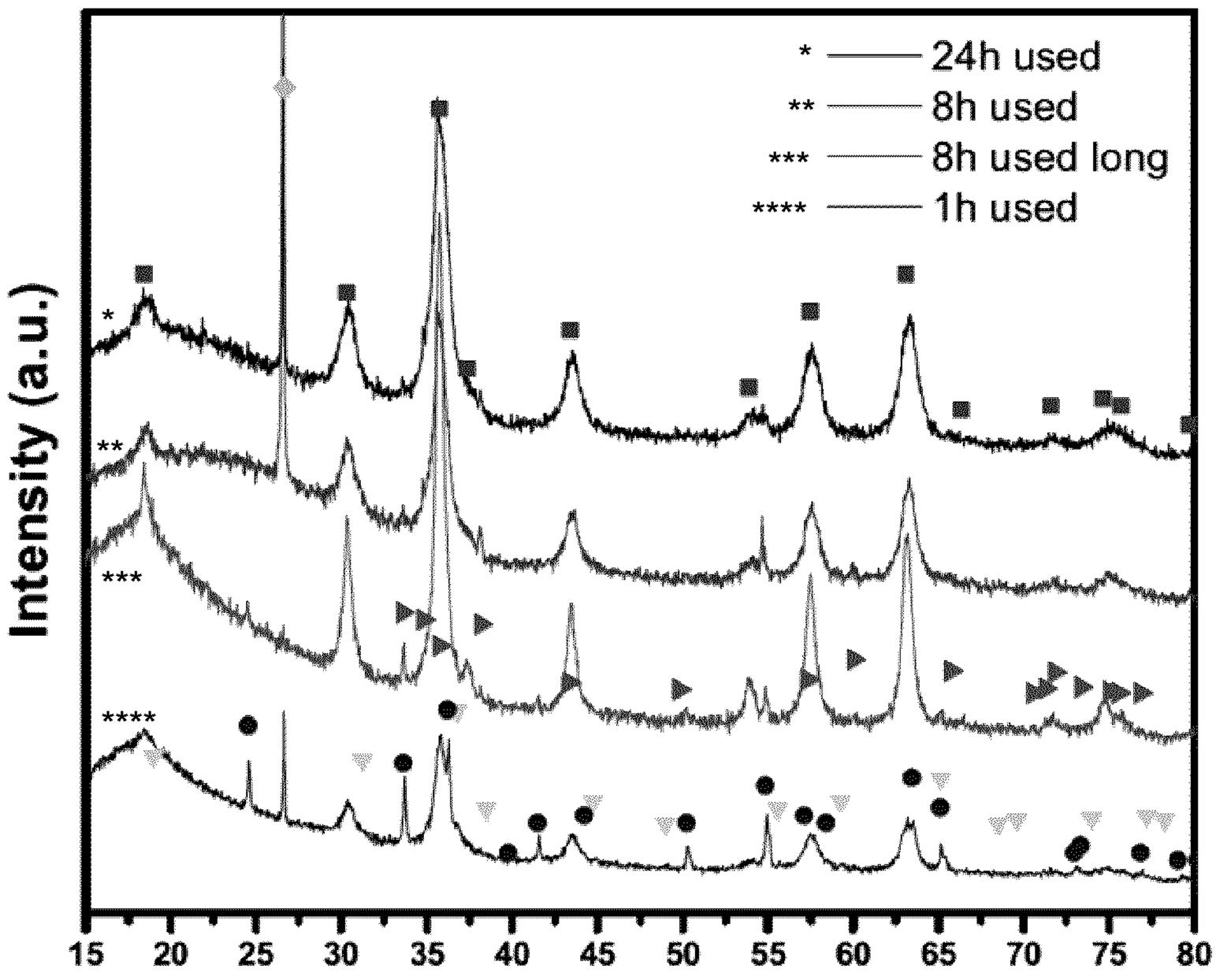

* 24h used
** 8h used
*** 8h used long
**** 1h used
Intensity (a.u.)
15 20 25 30 35 40 45 50 55 60 65 70 75 80
2-Theta (°)

FIG. 25

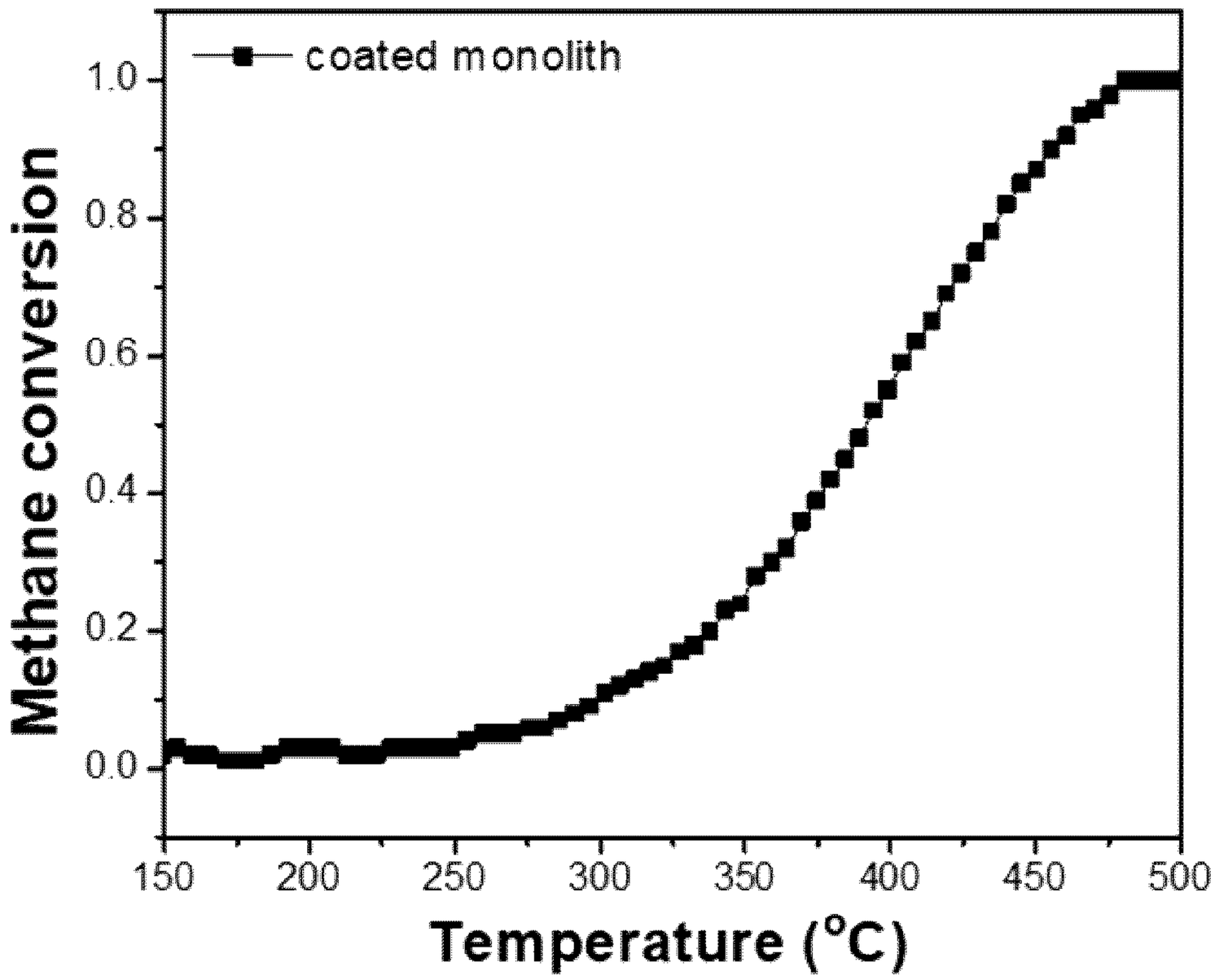

coated monolith
Methane conversion
0.0
0.2
0.4
0.6
0.8
1.0
150
200
250
300
350
400
450
500
Temperature (°C)

FIG. 26

INTERNATIONAL SEARCH REPORT

International application No.
PCT/CA2020/051603

A. CLASSIFICATION OF SUBJECT MATTER
IPC: **C01G 51/00** (2006.01) , ***B01J 37/02*** (2006.01) , ***B01J 37/08*** (2006.01) , ***C01G 37/14*** (2006.01) , ***F01N 3/28*** (2006.01) , ***F23C 13/08*** (2006.01)

According to International Patent Classification (IPC) or to both national classification and IPC

B. FIELDS SEARCHED

Minimum documentation searched (classification system followed by classification symbols)
C01G 51/00 (2006.01), B01J 37/02 (2006.01), B01J 37/08 (2006.01), C01G 37/14 (2006.01), F01N 3/28 (2006.01), F23C 13/08 (2006.01)

Documentation searched other than minimum documentation to the extent that such documents are included in the fields searched

Electronic database(s) consulted during the international search (name of database(s) and, where practicable, search terms used)
Questel-Orbit, Scopus, Google Patent/Scholar (cobalt chromite, CoCr2O4, nanoparticle, solvothermal)

C. DOCUMENTS CONSIDERED TO BE RELEVANT

Category*	Citation of document, with indication, where appropriate, of the relevant passages	Relevant to claim No.
X	Zákutná et al., "Hydrothermal synthesis, characterization, and magnetic properties of cobalt chromite nanoparticles", J Nanopart Res, (2014), 16:2251	1-31
X	Gotta et al., "Catalytic activity of substituted chromite spinels for the oxidation of methane emitted by CNG engines", 29th Meeting on Combustion, 2006 retrieved from: http://www.combustion-institute.it/proceedings/proc2006/documenti/Papers/02-04-gotta-022.pdf	23-50

☐ Further documents are listed in the continuation of Box C. ☐ See patent family annex.

*	Special categories of cited documents:	"T"	later document published after the international filing date or priority date and not in conflict with the application but cited to understand the principle or theory underlying the invention
"A"	document defining the general state of the art which is not considered to be of particular relevance	"X"	document of particular relevance; the claimed invention cannot be considered novel or cannot be considered to involve an inventive step when the document is taken alone
"D"	document cited by the applicant in the international application	"Y"	document of particular relevance; the claimed invention cannot be considered to involve an inventive step when the document is combined with one or more other such documents, such combination being obvious to a person skilled in the art
"E"	earlier application or patent but published on or after the international filing date	"&"	document member of the same patent family
"L"	document which may throw doubts on priority claim(s) or which is cited to establish the publication date of another citation or other special reason (as specified)		
"O"	document referring to an oral disclosure, use, exhibition or other means		
"P"	document published prior to the international filing date but later than the priority date claimed		

Date of the actual completion of the international search	Date of mailing of the international search report
23 December 2020 (23-12-2020)	05 February 2021 (05-02-2021)
Name and mailing address of the ISA/CA Canadian Intellectual Property Office Place du Portage I, C114 - 1st Floor, Box PCT 50 Victoria Street Gatineau, Quebec K1A 0C9 Facsimile No.: 819-953-2476	Authorized officer Stewart Parsons (819) 639-8528